



Arnold Schwarzenegger  
Governor

# SLAT-ARRAY CONCENTRATOR DEVELOPMENT

*Prepared For:*  
**California Energy Commission**  
Public Interest Energy Research Program

*Prepared By:*  
SVV Technology Innovations Inc.

PIER FINAL PROJECT REPORT

August 2009

CEC-500-2009-074



**Prepared By:**  
SVV Technology Innovations, Inc.  
Sergey Vasylyev  
Elk Grove, California 95757  
Commission Contract No. 500-00-034

**Prepared For:**  
Public Interest Energy Research (PIER)  
**California Energy Commission**

Hassan Mohammed  
**Contract Manager**

Kenneth Koyama  
**Office Manager**  
**Energy Generation Research**



Martha Krebs, Ph.D.  
**PIER Director**

Thom Kelly, Ph.D.  
**Deputy Director**  
**ENERGY RESEARCH & DEVELOPMENT DIVISION**

Melissa Jones  
**Executive Director**

## DISCLAIMER

This report was prepared as the result of work sponsored by the California Energy Commission. It does not necessarily represent the views of the Energy Commission, its employees or the State of California. The Energy Commission, the State of California, its employees, contractors and subcontractors make no warrant, express or implied, and assume no legal liability for the information in this report; nor does any party represent that the uses of this information will not infringe upon privately owned rights. This report has not been approved or disapproved by the California Energy Commission nor has the California Energy Commission passed upon the accuracy or adequacy of the information in this report.



## Acknowledgements

The research team would like to acknowledge the contributions of Dr. Viktor Vasylyev to the successful completion of this project. With his immense technical expertise in the areas underlying this research, he constantly provided the authors with fruitful ideas and timely advice. Thanks are also extended to the members of the Program Advisory Committee (PAC) and especially to Bruce Vincent and Joe McCabe for their valuable advice, criticism, and suggestions, which helped to deal with real world problems during the research. Finally, the team would like to thank dozens of residents of Sacramento, Davis, and Elk Grove who expressed support for the solar energy research and provided additional inspiration for the study.

Please cite this report as follows:

Vasylyev, Sergey. 2009. *Slat-Array Concentrator Development*. California Energy Commission, PIER Renewable Energy Technologies Program. CEC-500-2009-074



## Preface

The California Energy Commission's Public Interest Energy Research (PIER) Program supports public interest energy research and development that will help improve the quality of life in California by bringing environmentally safe, affordable, and reliable energy services and products to the marketplace.

The PIER Program conducts public interest research, development, and demonstration (RD&D) projects to benefit California.

The PIER Program strives to conduct the most promising public interest energy research by partnering with RD&D entities, including individuals, businesses, utilities, and public or private research institutions.

PIER funding efforts are focused on the following RD&D program areas:

- Buildings End-Use Energy Efficiency
- Energy Innovations Small Grants
- Industrial/Agricultural/Water End-Use Energy Efficiency
- Renewable Energy Technologies
- Environmentally Preferred Advanced Generation
- Energy-Related Environmental Research
- Energy Systems Integration
- Transportation

*Slat-Array Concentrator Development* is the final report for the SMUD ReGen project (Contract Number 500-00-034), conducted by SVV Technology Innovations Inc. The information from this report contributes to PIER's Renewable Energy Technologies program.

For more information on the PIER Program, please visit the Commission's website at <http://www.energy.ca.gov/pier> or contact the Energy Commission at 916-654-5164.



# Table of Contents

Preface .....	iii
Abstract .....	x
Executive Summary .....	1
1.0 Introduction .....	5
1.1 Background and Overview .....	5
1.2 Technical Objectives .....	5
1.3 Report Organization .....	6
2.0 Project Approach.....	7
2.1 Scope of Work.....	8
2.2 Design and Fabrication of Small Pilot-Prototype .....	8
2.2.1 Concentrator Adaptation for PVs .....	8
2.2.2 Development of Ray Tracing and Modeling Software .....	9
2.2.3 Development of Prototype Optical Configuration.....	12
2.2.4 Ray Tracing Analysis .....	13
2.2.5 Fabrication of Small Pilot-Prototype .....	15
2.2.6 Field Testing and Monitoring.....	21
2.3 Technical Feasibility Assessment.....	22
2.3.1 Test Setup .....	22
2.3.2 Methodology and Testing Procedures .....	24
2.3.3 Findings and Analysis .....	29
2.4 Design of a Commercial-Size Prototype .....	37
2.4.1 Design Improvement .....	37
2.4.2 New Optical Configuration .....	37
2.5 Fabrication of 30 ft <sup>2</sup> Prototype.....	38
2.5.1 Design and Fabrication of SAC Frame.....	38
2.5.2 Design and Fabrication of Test PV Receiver .....	40
2.5.3 Fabrication of Concentrator Slats.....	42

2.5.4 Assembling the Final Prototype.....	45
2.5.5 Monitoring and Evaluation of the Final Prototype .....	47
3.0 Project Outcomes .....	57
4.0 Conclusions and Recommendations .....	59
4.1 Conclusions.....	59
4.2 Commercialization Potential.....	59
4.2.1 Comparison to Parabolic Troughs .....	59
4.2.2 Comparison to Fresnel Lenses.....	64
4.3 Recommendations.....	65
4.4 Benefits to California .....	65
Nomenclature .....	67
References .....	69
Glossary .....	<b>Error! Bookmark not defined.</b> <a href="#">1</a>

## List of Figures

Figure 1. A 28-element Slat-Array Concentrator .....	7
Figure 2. A 3D computer model of the small SAC PV prototype .....	9
Figure 3. Data flow chart for ASCEND software .....	11
Figure 4. A screenshot of ASCEND software.....	11
Figure 5. CAM module with file export and template printout.....	12
Figure 6. Sunlight path for different optical concentrators.....	12
Figure 7. The irradiance distribution in the focal plane obtained from ray tracing .....	14
Figure 8. CNC machined brass molds .....	16
Figure 9. Non-vacuum thermoforming setup.....	16
Figure 10. Reflective slat reinforcement with aluminum coil.....	17
Figure 11. Finished support frame of the pilot CPV prototype.....	17
Figure 12. Concentrator solar cells for the initial CPV prototype .....	18
Figure 13. Aluminum extrusion heat sinks for CPV passive cooling .....	18

Figure 14. Finished PV receivers in operation .....	18
Figure 15. Two-axis solar tracker, illuminating receiver .....	19
Figure 16. Tracker support platform .....	19
Figure 17. Pilot prototype SAC, CPV system.....	20
Figure 18. A top view of pilot prototype .....	20
Figure 19. Modular PV receiver with series connected concentrator cells. ....	21
Figure 20. Remanufactured PV receiver with soldered contacts .....	22
Figure 21. A new five-cell PV receiver module .....	23
Figure 22. A single-cell reference PV module .....	23
Figure 23. A water-carrying chiller for the reference PV receiver .....	23
Figure 24. Concentrator test equipment .....	24
Figure 25. A screenshot of data acquisition and control software. ....	27
Figure 26. I-V curves measured for four different CPV .....	30
Figure 27. Power curves for the same PV receivers shown in Figure 26 .....	31
Figure 28. Selected I-V curves for different receiver modules.....	32
Figure 29. Power curve comparison.....	32
Figure 30. Experimental I-V curves for the reference receiver .....	33
Figure 31. Power curves for the reference receiver .....	34
Figure 32. Focal image and measured irradiance distribution in the focal spot.....	35
Figure 33. Irradiance distribution for a displaced receiver .....	36
Figure 34. Irradiance distribution comparison .....	38
Figure 35. Laser cut aluminum templates. ....	39
Figure 36. Improved Support Frame for 30- ft <sup>2</sup> Concentrator .....	40
Figure 37. A scheme of the new four-cells PV receiver. ....	41
Figure 38. Test receiver for the final prototype.....	41
Figure 39. Raw sheets of reflective material.....	42
Figure 40. An 8-foot adjustable shape template .....	43
Figure 41. Cylindrically curved slats fabricated for the final prototype .....	43

Figure 42. Tension-adjusted slat shape template.....	44
Figure 43. Slat lamination with a reflective film.....	45
Figure 44. The assembled final prototype in the upright position.....	45
Figure 45. The prototype SAC concentrator without film.....	46
Figure 46. The receiver support beam with a light scattering target.....	47
Figure 47. The final 30-ft <sup>2</sup> SAC prototype mounted on tracker.....	47
Figure 48. Solar radiation measurement and tracking sensors .....	48
Figure 49. The concentrator’s focal line .....	49
Figure 50. Digital CCD camera used for capturing focal images.....	50
Figure 51. Comparison of calculated (a) and actual (b) flux maps .....	51
Figure 52. Calculated (a) and actual (b) flux maps with focus improver.....	52
Figure 53. Test receiver based on high-efficiency PV cells.....	53
Figure 54. The concentrator designed to deflect wind loads .....	54

## List of Tables

Table 1. Concentration parameters obtained from ray tracing.....	15
Table 2. Concentrator optical efficiency estimated from $I_{sc}$ measurements.....	29
Table 3. Comparing measured and reference cell parameters. ....	34
Table 4. Comparison of measured and expected performance of PV .....	53
Table 5. PV Concentrator Technology Comparison.....	58

## Abstract

This project demonstrated a new technical solution for concentrating sunlight for photovoltaic (PV) power generation and solar thermal applications. The primary objectives were to design, build, test, and assess the performance of a new type of slat-array concentrator, a non-imaging blind-like reflector consisting of an array of inclined reflective slats positioned to redirect the incident solar radiation to a common linear focus.

By using an array of reflective slats, the weight and cost of the concentrator was reduced, and the concentrated sunlight was evenly distributed across the PV cells. As a result, when high-efficiency concentrated photovoltaic (CPV) cells are employed and the system is installed on a sun-tracking platform in an area with a high level of sun exposure, the efficiency of solar to electric energy conversion can be increased by more than 50 percent, compared to a fixed-position, flat-plate PV panel. The results of this project suggest advantages for the slat array concentrator over other concentrating technologies. These advantages include: outstanding flux uniformity, flexibility of concentration magnifications for various applications, simplicity of manufacturability, lowered weight, less wind loading, more capacity on a tracker, safer off-focus peak concentrations, breakage confined to an individual slat, and shorter focus advantages for solar thermal applications. This report describes the technical achievements realized in this project.

**Keywords:** Photovoltaics, solar concentrator, concentrating photovoltaics, concentrating solar power, distributed power, optical efficiency, solar to electric conversion efficiency, non-imaging optics, slat-array concentrator, PV, CPV



# Executive Summary

## Introduction

This project developed a potentially more-efficient concentrating photovoltaic (PV) system. This entailed designing and building a novel solar collector—called the *slat-array concentrator*—and demonstrating its feasibility.

This report summarizes and describes the key technical achievements of this project. The slat-array concentrator, once commercially available, may improve the economics of future solar-concentrating generation systems as well as concentrating solar thermal applications.

## Objectives

The technical goals of this project were to:

- Develop the software needed to analyze the optics of the slat-array concentrator.
- Improve reflective optics for solar concentrators by designing the slat-array concentrator and adapting it for uniform illumination of photovoltaic cells at moderate sunlight concentrations.
- Develop and test novel slat-array concentrator prototype modules.

To achieve these goals, the following objectives were set:

- Determine the technical and economic feasibility of fabricating a concentrating PV module based on the slat-array concentrator.
- Extensively test a small demonstration concentrating PV module.
- Design and build a 500 watt (W) slat-array module capable of generating electricity with 50 to 100 percent improved optical efficiency as compared to conventional parabolic mirror systems, while using 30 to 50 times less square footage of solar cells as compared to conventional flat plate solar panels and having less sensitivity to tracking error than other concentrating PV designs.

## Outcomes

This project integrated scientific concepts into an interactive software program that evaluated reflective geometries for solar concentrators. After input of correct parameters, the software produced a computer-integrated manufacturing file that was used to build the first slat-array prototype via a computer integrated manufacturing tooled model shop. The program developed several creative manufacturing scenarios using simple techniques and using a variety of available cheap materials for the slats, the supporting structure, and the PV receiver. Throughout the assignment the project team made slight design improvements to improve manufacturability and enhance the performance of the slat-array concentrator.

Simultaneous electrical and optical testing of prototypes confirmed the performance predicted by the simulations. The team found concentrator tolerances to be less critical than those of parabolic

concentrators. This may yield lower-cost concentrators that are easier to manufacture, install, and operate. The 0.5 kilowatt (kW) prototype, with improved focusing characteristics, demonstrated advantages over other solar concentrating technologies.

Demonstrated advantages include:

- High optical efficiency.
- Reduced weight.
- Less sensitivity to tracking errors.
- Lower potential manufacturing cost.

The project developed a new ray tracing and modeling software that the project team used to design custom slat-array concentrator optics and concentrated PV modules. Ray tracing is an advanced technique, in computer graphics, for adding realism to an image by including variations in shade, color intensity, and shadows that would be produced by having one or more light sources.

The slat-array concentrator, composed of an array of simple concave slats, had a high optical efficiency and performed in a manner similar to parabolic mirrors, which are today's most cost-effective solar concentrators. Comparing the slat-array prototypes to parabolic-mirror concentrators, weight was reduced, suggesting significant potential for lower manufacturing and installation costs. The project team obtained a world record low weight of about 10 kg/m<sup>2</sup> (2.5 lbs/ft<sup>2</sup>) for the slat-array modules.

The project achieved a concentration ratio of at least 40 suns with the slat-array prototypes, which is approximately twice the practical limit of current Fresnel lens-based solar concentrators. PV cell area was 30 to 35 times smaller than the area flat-plate PV panels of equivalent power output.

Excellent uniformity of concentrated flux was obtained without the use of secondary optics. At 20 suns of concentration, the flux irregularities did not exceed 10 percent of the targeted concentration. Concentrator optical efficiencies were 85 to 89 percent with a material reflectance of 89 to 92 percent.

In summary, the project demonstrated that very simple reflector shapes using commercially available reflective materials based on aluminum substrate with conventional sheet metal fabrication techniques can be used for manufacturing high-flux solar concentrators.

### **Technical Objectives**

Demonstrating the technical feasibility of the slat-array concentrator concept was the primary goal of this project, and this was accomplished by:

- Creating a software package that: (1) successfully showed the capabilities of the slat-array concentrator; and (2) incorporated design improvements in the demonstrations.
- Testing of the new slat-array design by building two demonstration modules. The first was a small, first-of-its-kind, slat-array module used to validate the design. The second

was a 2.79 m<sup>2</sup> (30 ft<sup>2</sup>) 500 W slat-array concentrator module. This module will serve as a prototype for future commercial slat-array concentrator systems.

Modeling and experimental data gathered in this project provided valuable information regarding the optical performance of the slat-array concentrator as well as other technical characteristics.

### **Conclusions**

The technical performance demonstrated by the slat-array concentrators in this project shows that this technology offers technical advantages in the collection and use of solar energy. Forty suns of optical concentration, obtained by the small prototype, is in agreement with the performance goals set at 30 to 50 suns concentration. This is accomplished without overheating the central portions, or any portion, of the cells.

The large 500 W prototype module demonstrated the ability of the slat-array concentrator concept to produce highly uniform concentrated fluxes while maintaining high concentration with design and manufacturing simplicity. The 500 W concentrated PV prototype demonstrates the potential for future commercial systems producing distributed electrical power.

### **Recommendations**

A further refinement of the slat-array concentrator concept is needed to fully exploit its benefits and determine its limits. With additional development and demonstrations, the solar industry could create a robust commercial product that will incorporate the best possible slat-array concentrator fabrication technologies, a suitable PV receiver, and a matching sun tracking system. It is probable that slat-array concentrators will be well-suited for solar thermal applications and systems of this type should be designed and demonstrated.

### **Benefits to California**

This project provides significant value to California by developing a new low-cost renewable generation technology for tomorrow's electricity system. The slat-array concentrator developed and demonstrated in this project has an installed weight equal to a flat-plate PV module, while providing 20 to 40 times reduction of PV cell surface area and a corresponding reduction in silicon usage.

SVV Technology Innovations, Inc., is working to develop this technology to expand the PV market by providing a lower-cost alternative to conventional and emerging concentrated PV technologies. Further development of this technology will yield solar concentrators that should cost less and be easier to maintain than existing concentrator technologies. This will help the PV industry meet its goal of developing low-cost technologies suitable for use in a wide range of distributed-generation applications.

Future products based on the slat-array concentrator, such as solar thermal collectors, water heaters, desalinators, and chillers, will become more effective and more marketable as the slat-array concentrator develops. California's electric ratepayers will benefit from the increased

amount of electricity generated from renewable sources, reducing the peak demand for grid-supplied electricity and the likelihood of electricity shortages.

## 1.0 Introduction

Photovoltaic (PV) cells are solid-state semiconductor devices primarily made of purified silicon that convert light energy into electric current. The abundance of silicon material and the maturity of PV cell manufacturing processes make PVs an important technology to address the growing demand for nonpolluting electricity generation from renewable sources. However, the high cost and limited availability of the high-purity silicon used for PV cell production has been a major obstacle to increasing market adoption.

The use of systems to concentrate solar radiation before directing it to the PV cells can potentially reduce the overall cost of solar power generation. The per-area cost of most of today's solar thermal-to-electric concentrators can be several times less than that of flat plate PV panels. Since the power output of quality PV cells is normally proportional to the incident flux density, higher concentration ratios proportionally reduce the need for PV materials, resulting in cost savings. Concentrated PV (CPV) is an emerging technology that could allow the industry to exploit the benefits of PV while lowering the cost of PV electricity generation.

### 1.1 Background and Overview

There are two established approaches for concentrating the solar energy to relatively high levels suitable for CPVs: parabolic mirrors and Fresnel lenses. Parabolic mirrors have a much better concentrating ability and can be made in larger sizes than Fresnel lenses. However, parabolic systems have tight optical-quality fabrication and expensive support frames, two factors that increase the cost of such systems. The optical and stability requirements of the mirror lead to a significant increase in system weight and cost which diminishes the advantage of concentration. Fresnel lenses offer a greater convenience for system design and operation. However, Fresnel lenses are limited in size and concentration ratio.

Both established concentrator approaches are better suited for solar thermal applications than PV, because they produce hot spots on target PV cells due to a non-uniform spread of the concentrated solar flux. The hot spots often contribute to notable decreases in PV cell performance, decreases in product life expectancy, and failures.

In order to be competitive in the power-generation market, the concentrators must be lightweight and low-cost, while retaining high sunlight collection efficiency. Under this project, the authors studied a breakthrough technical approach using non-imaging reflective lenses. A decade of prior work by the authors preceded the development of the prototypes funded in this project.

The slat-array concentrator developed in this project represents a new optical design for solar concentrators, taking the capabilities of traditional concentrating collectors beyond those of parabolic mirrors and lenses, and offering the potential of significantly lower cost per unit area.

### 1.2 Technical Objectives

The overall goal of this project was to demonstrate a new technical solution, the slat-array concentrator (SAC), for concentrating sunlight for distributed power generation using PVs and

solar thermal applications. The main project objective was to design, build, and evaluate two prototype slat-array concentrators. This project was a proof-of-concept demonstration of the high-flux solar collector, based on a back-focus, reflective latticework used in place of a conventional parabolic mirror or Fresnel lens.

The secondary goals of this project were to:

1. Significantly improve the practicality of reflective optics for solar concentrators by introducing a new lens-like reflective concentrator concept (the slat array concentrator) and adapting it for uniform illumination of PV cells or other receptors at moderate sunlight concentrations.
2. Develop and test a novel CPV prototype module employing the slat-array concentrator design, with increased optical efficiency, and the possibility of lower installation and operating costs.

To achieve these goals, the following technical objectives were set:

1. Determine if it is technically and economically feasible to fabricate and use a CPV module based on the slat array lens-like reflective optics.
2. Validate the novel CPV design against existing flat-plate and concentrator PV modules.
3. Establish a 500 W system design generating electricity with 50 to 100% improved optical efficiency compared to parabolic mirror systems.
4. In the 500 W prototype, utilize 30 to 50 times less square footage of solar cells as compared to conventional flat plate solar panels.
5. Have reduced tracking requirements compared to other CPV technologies.

### **1.3 Report Organization**

Section 2.0 describes: (1) the project's scope-of-work; (2) the design and development of the prototypes; (3) the fabrication of the prototypes; and (4) the testing, analysis, and evaluation of the prototypes. Additionally, Section 2.0 describes the development of the larger scale prototype based on design improvements from the initial pilot prototype. Section 3.0 reports on the project outcomes. Section 4.0 discusses the conclusions and recommendations.

## 2.0 Project Approach

The slat-array concentrator is a non-imaging, Venetian blind-like reflector consisting of an array of inclined reflective slats positioned to redirect the incident solar radiation to a common linear focus.

There are some apparent similarities between the slat-array concentrator and a conventional linear-focus Fresnel mirror in the way the reflector is designed. Both are composed of an array of straight and relatively narrow slats made of a reflective material and aligned along the focal line. However, the reflective slats of the slat-array concentrator are inclined at sharper angles with respect to the incident solar flux and positioned closer to each other. Due to the special alignment of slats in the slat-array concentrator, the incident solar flux is split into multiple convergent beams that are directed not upward but downward through spaces between the adjacent slats, using only a single stage of reflection and reduced energy losses.

The slat-array concentrator is a purely reflective system, having the isolated focus behind the reflection, distinguishing its design from any other available high-flux reflectors. In the past, back focus has been considered an attribute of refractive lenses only. This concentrator incorporates any convenient number of slats and modifies to create high-intensity solar radiation fluxes in a wide range of concentrations, roughly from 10 to 200 suns. Figure 1 shows an example of slat-array concentrator composed of 28 concave slats, with two symmetrical wings and designed for about 160-sun geometrical concentration.

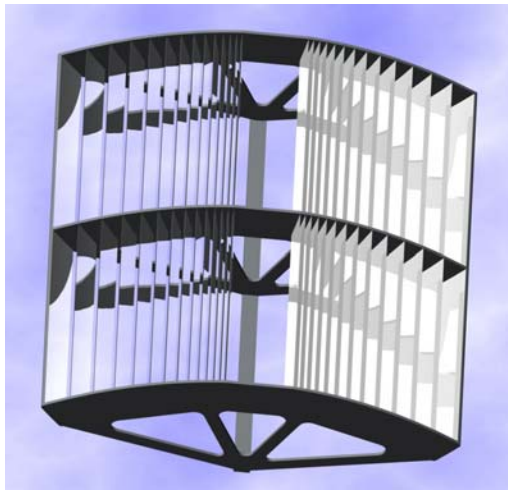


**Figure 1. A 28-element slat-array concentrator**

Photo Credit: SVV Technology Innovations

Besides providing a rear focus, which allows one to place the energy receiver/converter without interrupting the solar flux, the slat-array concentrator brings a new dimension to solar collector optics with its ability to adapt the focal spot for particular applications. This feature can be extremely useful for concentrating PV since the performance of most PV cells is vulnerable to inconsistencies of the concentrated beam. Individual slats can be designed in such a way that

their respective focal spots are slightly offset relatively to each other, thus the uniformity of the concentrated beam can be improved. These findings led the project team to design and develop a slat-array CPV module which could serve as a prototype for future low-cost CPV systems.

## **2.1 Scope of Work**

The following tasks were designed to accomplish the objectives of this project:

- Design and Fabricate Small Pilot-Prototype—Develop a physical model of asymmetric, low-profile, non-imaging concentrator, optimized for uniform cell illumination and moderate concentrations; select system parameters from ray tracing simulation, procure materials and equipment; acquire materials; fabricate components; and assemble the module with 0.14 m<sup>2</sup> (1.5 ft<sup>2</sup>) working aperture.
- Assess Design Feasibility—Conduct literature research on existing data correlations, assemble experimental setup, conduct extensive system measurements, analyze test results, perform feasibility analysis, and prepare the working pilot-prototype for demonstrations.
- Plan CPV Fabrication—Using the results of the pilot-prototype, revise and improve the SAC design; develop model for scaling; acquire materials: high-performance PV cells, solar tracker, and other equipment; and design a 500 W prototype system.
- Fabricate Commercial-Size Prototype—Fabricate components and assemble a prototype module with 2.79 m<sup>2</sup> (30 ft<sup>2</sup>) working area, measure power output of the prototype under normal conditions, develop recommendations for industrial manufacturing and further commercial use of the system, prepare and submit the final report.

## **2.2 Design and Fabrication of Small Pilot-Prototype**

### ***2.2.1 Concentrator Adaptation for PVs***

The slat-array concentrator concept is well suited for the manufacturing of concentrator PV devices that are modular and inexpensive. The development of a prototype CPV module benefited from the high concentration ability of the slat-array concentrator. This allowed the authors to further simplify the slat-array concentrator design by utilizing an asymmetric version of the concentrator. Using customized software, different reflective slat arrangements were reviewed and a final design selection was made.

Based on a comparative study of different curved profiles for the slats, the research team selected circular profiles. Despite the fact that the circular shapes were found to be less efficient in concentration when compared to the parabolic ones, circular shapes are easier to manufacture and achieve better concentrated flux uniformity than parabolic shapes.

The authors determined that, within this scheme, the individual circular profiles can deliver 6 to 11 suns concentration each, resulting in the theoretical maximum of about 70 suns for the selected design. Given the anticipated surface and shape imperfections, the target concentration ratio for the SAC was established at around 40 suns.

The research team designed a small concentrator CPV module based on the modified slat-array concentrator. The design included a built-in concentrator support frame, also suitable for supporting a linear array of concentrator cells. An extruded heat sink, for passive PV cell cooling, is shown on the lower left side of the rendering in Figure 2.

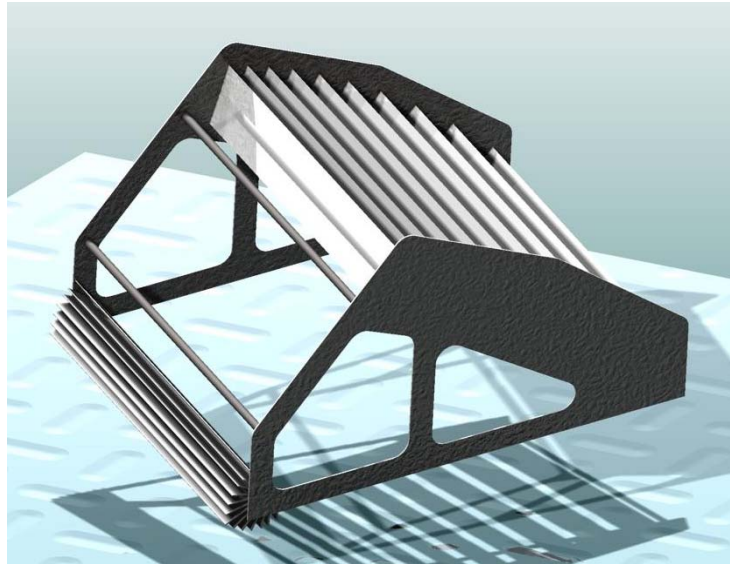


**Figure 2. A 3D computer model of the small SAC PV prototype**

Photo Credit: SVV Technology Innovations

### **2.2.2 Development of Ray Tracing and Modeling Software**

The slat-array concentrator is based on a unique optical concept that initially posed difficulties in finding a suitable software tool for design modeling and ray tracing analysis. Initially, the project team used proprietary ray tracing software, developed earlier by the project authors, to develop a preliminary optical scheme for the low-profile, asymmetric concentrator design shown in Figure 2. This scheme included 10 inclined slats ranging from 8 to 11 centimeters (3.15 to 4 inches) in width and having a length of 40 cm (15.75 in). The desired size of the prototype concentrator was defined to be 40 × 40 cm (15.75 × 15.75 in) including a 0.16 m<sup>2</sup> (1.7 ft<sup>2</sup>) active aperture area.

New analytical features were required for the software to be able to arbitrarily alter the SAC design to meet concentrated flux uniformity objectives. For this purpose, a new computer program, ASCEND, was designed and developed. It used many of the algorithms of the research team previous ray tracing program and added a number of interactive and visualization features needed for the CPV design.

The following four main modules were implemented in ASCEND's software as shown in Figure 3:

1. Baseline design input module—Utilizes pre-calculated model-based concentrator configurations as the initial input, for further modification in accordance with the design requirements.

2. CAD module—Provides software means for manual and semi-automatic tailoring of the dimensional parameters of individual slats and the PV receiver. Supports direct editing of the position and shape characteristics, as well as drag-and-drop, resize, rotate, copy/clone and other operations. Figure 4 shows an example of the program CAD module graphical user interface.
3. Control and visualization module—Performs most of the calculations and allows visualization and numerically control over the results of concentrator designed by the CAD module.
4. The following characteristics of the concentrator and the receiver zone are calculated and displayed:
  - a. Concentrator active aperture.
  - b. Raw geometric concentration obtained from the edge-ray estimation.
  - c. Concentration ratios and corresponding receiver widths for 100%, 90%, and 80% of the incident solar rays, respectively: 100% “ideal” reflection is assumed for all calculations.
  - d. Zoomed plot of edge ray distribution in the receiver vicinity.
  - e. Spatial distribution of rays in the concentrated flux created by a cross-section of the concentrator.
  - f. Plot of the expected energy distribution on the target PV panel in 2D or 3D.
5. Input/output module—Provides save/load and export/import capabilities so that the design can be saved in an internal *slt* format for continuing the work later, or exported into an external file for exchanging with other application or manufacturing purposes. The I/O module also provides some basic computer aided manufacturing (CAM) features to assist in slat manufacturing. It allows for viewing/exporting the cross-sectional dimensions of each slat (Figure 5), as well as generating a template printout for a selected profile.

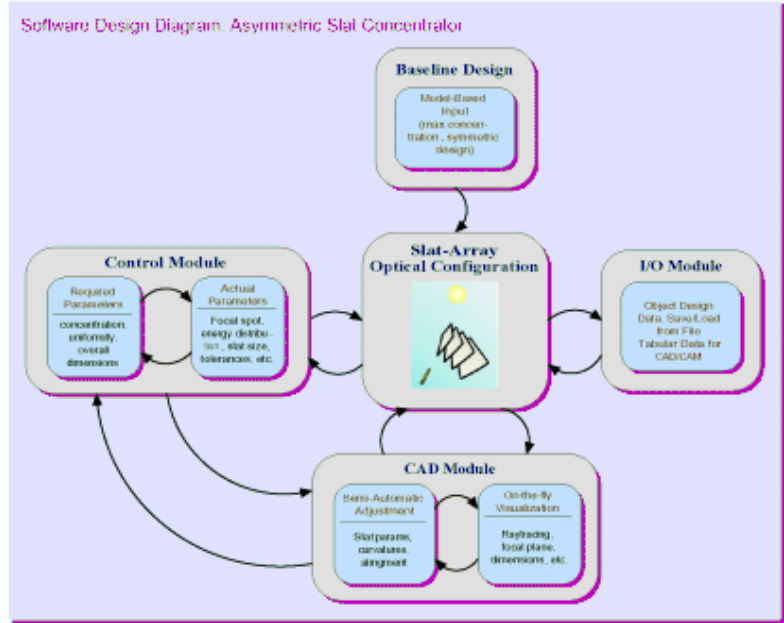


Figure 3. Data flow chart for ASCEND software

Photo Credit: SVV Technology Innovations

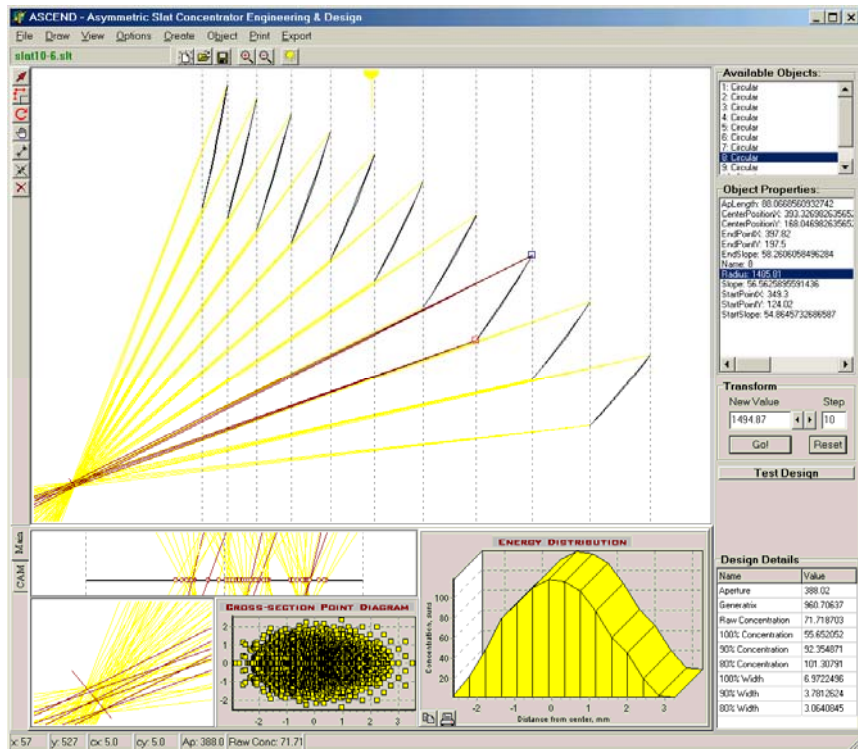
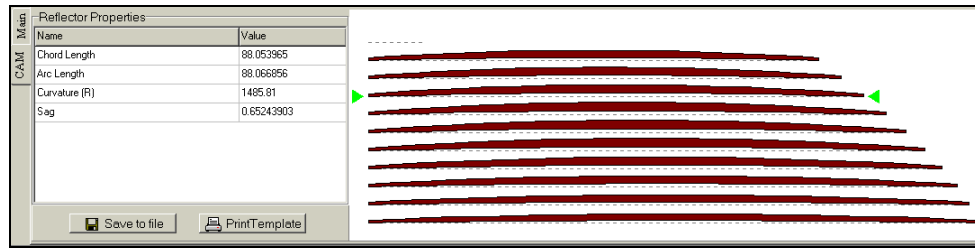


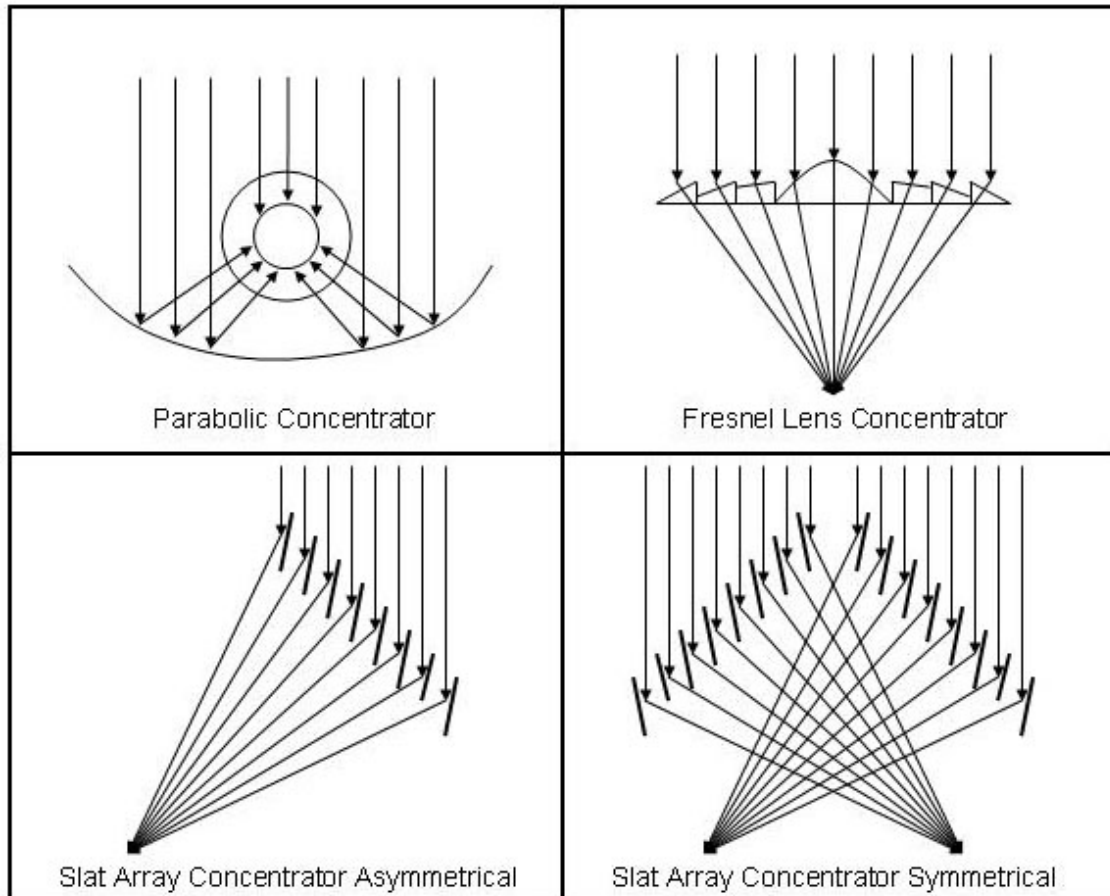
Figure 4. A screenshot of ASCEND software

Photo Credit: SVV Technology Innovations



**Figure 5. CAM module with file export and template printout**

Photo Credit: SVV Technology Innovations



**Figure 6. Sunlight path for different optical concentrators.**

Photo Credit: SVV Technology Innovations

### **2.2.3 Development of Prototype Optical Configuration**

The ASCEND software was used to further optimize the concentrator’s optical configuration for a centimeter-wide PV receiver, and calculate the concentration and dimensional parameters of the prototype CPV device.

In the optimized design, 7 out of 10 slats were identical to each other, to simplify the manufacturability, while maintaining the collection efficiency and uniformity of the concentrated sunlight. The other three slats were the same size, with only a small difference in curvature. A relatively low system profile, with a concentrator’s focal distance to active aperture ratio of about

0.74, was achieved. This aperture ratio is less than other CPV systems based on parabolic troughs and Fresnel lenses. For comparison, Figure 6 shows the sunlight paths in the parabolic trough, Fresnel lens, asymmetrical and symmetrical slat-array concentrator developed in this project.

### 2.2.4 Ray Tracing Analysis

Ray tracing with ASCEND was carried out based on geometric optics, using the following assumptions:

- The operating conditions were assumed to be ideal, including 100% specular reflectivity of the reflective slats and negligible losses on the receiver.
- The incident radiation flux was considered to be uniformly distributed on the entrance aperture of the concentrator.
- The direct sunlight was simulated by a large number of rays quasi-uniformly distributed within a cone of an opening equal to the angular size of the sun (32 arc min or 0.53 degrees).
- Movements of the concentrator were simulated by changing the direction of the incident flux.

Solar limb darkening for direct spectrum was taken into account as the brightness  $B$  varies in accordance with the empirical relation of limb darkening which, in turn, depends on the positional angle of the sun  $\theta_p$  and can be derived from an empirical relation for maximum spectral brightness:

$$B = B_0 (0.35 + 0.65 \cos \theta_p) \quad (1)$$

On the other hand,  $\theta_p$  relates to the angular distance  $\theta_c$  from the direction to the sun as,  $\sin \theta_p = \frac{\sin \theta_c}{\sin \phi_{SUN}}$  where  $\phi_{SUN}$  is the angular size of the sun.

Accordingly,

$$B(\theta_c) = B_0 \left( 0.35 + 0.65 \sqrt{1 - \frac{\sin \theta_c}{\sin \phi_{SUN}}} \right) \quad (2)$$

The geometrical concentration is defined as:

$$C_G = \frac{A_C}{A_R}, \quad (3)$$

where  $A_C$  and  $A_R$  are the entrance apertures of the concentrator and the receiver, respectively.

Raw concentration  $C_{RAW}$  is defined from the edge-ray method as the ratio of the concentrator entrance aperture to the focal spot size constrained by the uttermost (in the cross-section) rays emanating from the opposite edges of the solar disk.

In the following material, we will use the concept of intercept factor (IF). IF is determined by the percentage of incident rays intercepted by the receiver of a pre-defined width. A 100% IF corresponds to the entire incident flux (100% incident rays) so that  $C_G$  can be found to be simply a ratio of total concentrator aperture to the receiver aperture.

In the process of design optimization, a number of parameters were controlled through the ASCEND program, including the raw concentration  $C_{RAW}$  of individual slats and the entire concentrator, geometric concentration  $C_G$  for 70%, 80%, 90%, and 100% intercept factors, a degree of degradation of respective values against the slat/concentrator misalignment and displacement, and all key dimensional parameters. In order to generate a cross-sectional “slice” of concentrated flux, an array of up to 1,000,000 artificial incident rays originating from 100 points equidistantly positioned on the concentrator’s surface was used.

Figure 7 shows the calculated energy distribution obtained from ray tracing for an ideal slat-array PV concentrator and a flat linear receiver.

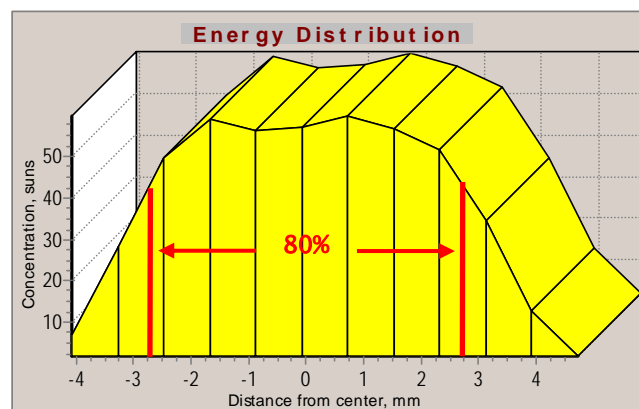


**Figure 7. The irradiance distribution in the focal plane obtained from ray tracing**

Photo Credit: SVV Technology Innovations

The ray tracing analysis shows that the selected arrangement of concentrator slats results in the net geometrical concentration ratio of about 40 suns for a 1 cm (0.4 in) linear receiver, as well as a uniform distribution of the concentrated flux over most of the PV receiver area.

Table 1 shows the concentration parameters for different IF. While the net geometrical concentration ratio corresponding to a 100% IF is almost 40 suns, the respective concentrations for 90% of incident flux or less are well above 50 suns. This means that, in a real concentrator employing the current optical configuration and quality reflective slats, uniform-flux concentrations of 40 to 50 suns can be reached with minimum energy loss. The results from ray tracing demonstrate how the hot spots in the PV receiver center can be eliminated by using the SAC approach.

**Table 1. Concentration parameters obtained from ray tracing**

<i>Intercept Factor</i>	<i>Concentration, suns</i>	<i>Receiver width, mm/in</i>
100%	38	10/0.4
90%	54	6.4/0.25
80%	56	5.4/0.21

Source: Data collected by Sergey Vasylyev

## **2.2.5 Fabrication of Small Pilot-Prototype**

### ***Fabrication of SAC Reflectors***

One experimental method of the concentrator's slat fabrication included non-vacuum thermoforming from plastic materials. This method used 7.61 cm (3 in)-wide strips cut from a 0.16 cm (1/16 in) acrylic sheet. Each acrylic strip was laminated with a self-adhesive reflective film.

The required shape for the slats was obtained by bending the strips to an appropriate radius, using a computerized numerical control (CNC) machined cylindrical mold at an elevated temperature. Figure 8 shows the molds representing the four different circular profiles of concentrator slats.

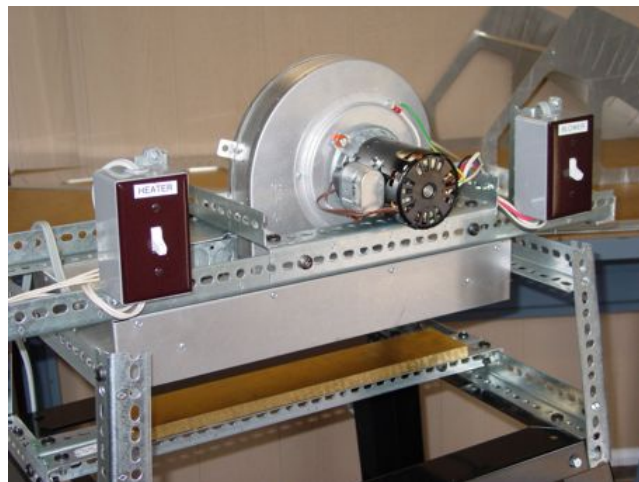
In an effort to add rigidity to the reflector, different types of slat reinforcement were evaluated. Acceptable results were obtained with plastic stiffening ribs and slat reinforcement using a mesh filler and epoxy compound. Despite the fact that the required shape tolerances were obtained with plastic slats, the long-term shape stability still remained a concern. Therefore, the project team decided to focus on slat fabrication from aluminum sheet materials.



**Figure 8. CNC machined brass molds**

Photo Credit: SVV Technology Innovations

The required thermoforming temperature was provided by a simple thermoforming setup including a 2-kW perforated ceramic panel heater with a blower attached for improved air convection and uniform heating (Figure 9).



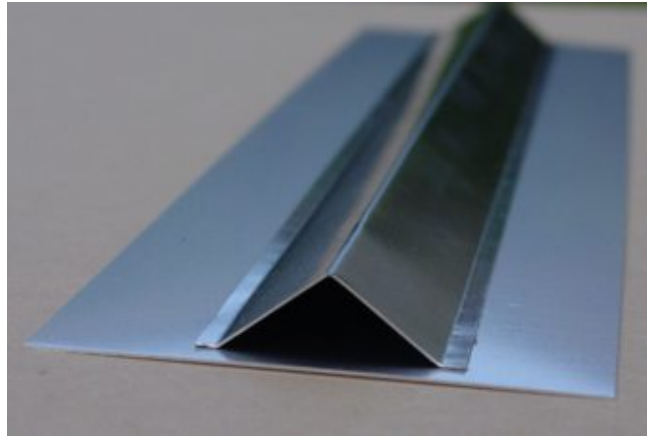
**Figure 9. Non-vacuum thermoforming setup**

Photo Credit: SVV Technology Innovations

After testing different approaches, the research team selected a commercially available, highly reflective aluminum laminated with a protective plastic film. The required shapes for the slats were obtained using a simple technique. Each slat, essentially a reflective strip pre-cut from a raw sheet of the reflective aluminum, was clamped between two thin aluminum plates and passed through a bench-top slip rolling machine. The slat shape was controlled by a radius template, as well as by checking its focal distance under sunlight exposure.

Appropriate slat thickness and structural reinforcement methods were also a subject of experimentation. The radius of curvature of concentrator slats is fairly large. This makes them almost flat in appearance. They are subject to bending in a longitudinal direction under their own weight if not enough material thickness is provided. A 0.5mm (0.02 in) slat reinforced by a

stiffener made of lightweight aluminum coil was attached to the slat's back side with an adhesive transfer tape. This combination provided enough stiffness while keeping the overall weight of slats fairly low. The stiffeners were designed to fit the shadow zones between the concentrator slats, making sure that no solar flux blocking occurred. Figure 10 shows a finished slat.



**Figure 10. Reflective slat reinforcement with aluminum coil**

Photo Credit: SVV Technology Innovations

### ***Fabrication of CPV Support Frame***

The slats were secured between two identical walls made of 0.1524 cm (0.06 in) aluminum sheets in which appropriate circular-profile slots were laser cut to hold the slat ends. The sidewalls were fabricated with the use of the ASCEND program, outputting a CIM file to a fabricator. The finished aluminum walls were fastened to each other by lightweight aluminum tubes to form a rigid open-frame structure (Figure 11).



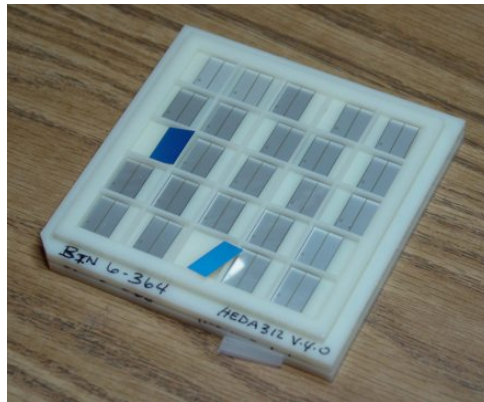
**Figure 11. Finished support frame of the pilot CPV prototype**

Photo Credit: SVV Technology Innovations

### ***PV receiver***

Originally, we planned to utilize monocrystalline silicon cells, designed for up to 40 suns concentration and utilized in several European CPV demonstrational projects. However, we discovered that this type of cell has been discontinued by the manufacturers.

Therefore, we decided to utilize another type of concentrator cell, produced in California. We acquired a set of bare cells to fabricate test receivers for the original CPV prototype. These dense-array cells (shown in Figure 12) have dimensions of  $1 \times 1.5$  cm ( $0.4 \times 0.6$  in), and can operate at concentration ratios of up to 300 suns, which provided enough dynamic range for the proof of concept testing of about 40 suns concentration.



**Figure 12. Concentrator solar cells for the initial CPV prototype**

Photo Credit: SVV Technology Innovations

The cells were initially connected in a series using self-adhesive copper strips, and mounted on an extruded aluminum heat sink using a thermal conductive tape. Figures 13 and 14 show heat sink modules before and after mounting the PV cells.

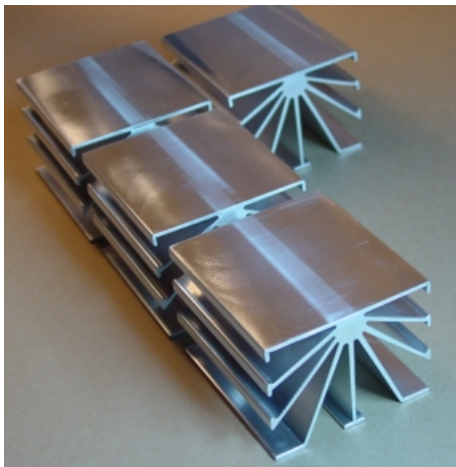


**Figure 13. Aluminum extrusion heat sinks for CPV passive cooling**

Photo Credit: SVV Technology Innovations

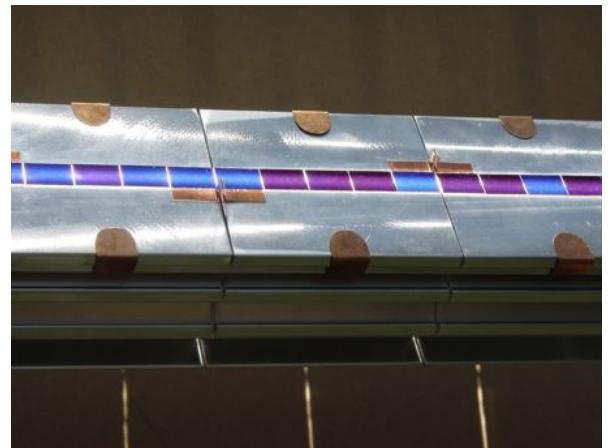


**Figure 14. Finished PV receivers in operation**

Photo Credit: SVV Technology Innovations

## **Solar Tracker**

A commercial two-axis solar tracker (Figure 15) was attached to a mobile platform which included a pipe mast and a steel-welded frame for supporting the tracker (Figure 16). The gear drive of the tracker allowed it to automatically track the sun by rotating the CPV prototype up to 270 degrees and tilting it 5 to 75° for elevation. It also allowed for manual tracking control when needed. Figure 15 shows the pilot prototype mounted on the tracker, brightly illuminating the receiver with concentrated sunlight.

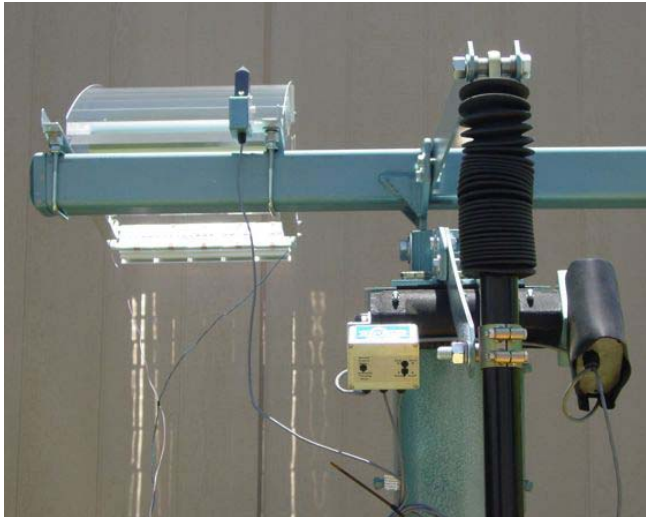


**Figure 15. Two-axis solar tracker, illuminating receiver**

Photo Credit: SVV Technology Innovations



**Figure 16. Tracker support platform**

Photo Credit: SVV Technology Innovations

## **Assembling the pilot prototype CPV**

The first CPV prototype based on the slat-array concentrator with the active aperture of about 0.16 m<sup>2</sup> (1.7 ft<sup>2</sup>) was assembled and mounted on the tracker for concentrator concept verification and monitoring. Figures 17 and 18 show different views of the pilot-prototype. In Figure 18, the dark blue horizontal strip seen in the center slat of the SAC is a magnified reflection of the PV receiver, seen at the bottom of the picture without magnified reflection.



**Figure 17. Pilot prototype SAC, CPV system**

Photo Credit: SVV Technology Innovations



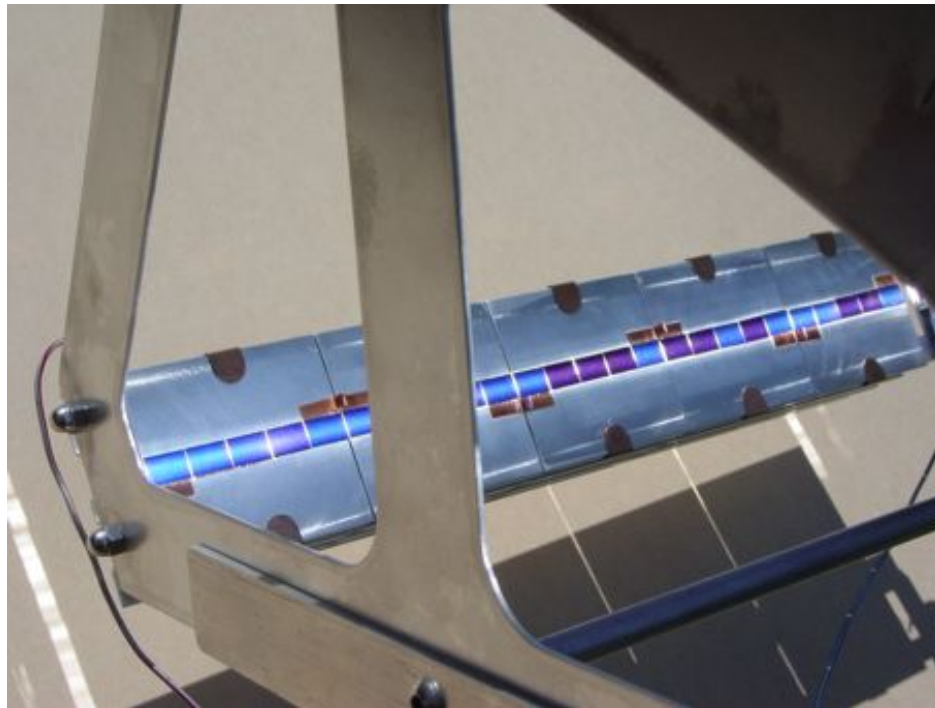
**Figure 18. A top view of pilot prototype**

Photo Credit: SVV Technology Innovations

## 2.2.6 Field Testing and Monitoring

### Initial Monitoring

The CPV system was monitored to confirm its performance. It was run continuously for 5 to 8 hours a day, under the direct sunlight exposure, for a 10-day period in Davis, California. A closer view of the PV receiver is shown in Figure 19. As the picture shows, the focal line occupies the entire receiver's width, corresponding to a solar flux intensification of about 40 suns.



**Figure 19. Modular PV receiver with series connected concentrator cells.**

Photo Credit: SVV Technology Innovations

The monitoring routine included checking the stability of the concentrator's focus, the temperature regime of the cells, and the basic electrical characteristics of the sample receiver module. The system was also checked for the presence of any degradation of prototype components.

The concentrator performed well during this short period, and no degradation of either slat shapes or their reflective surfaces was observed. Some deposition of dust and other air contaminants were easily removed with water and a generic lens cleaning solution.

The concentrating PV receiver did cause some problems. While performing flawlessly under smaller concentrations and in a resistor shunted circuit, one or more cell interconnections repeatedly failed under the full concentration in the open circuit measurement mode. Repairing the failed receiver modules and replacing the cells did not permanently solve the problem. After investigation, we identified the problem as being related to the electro-conductive acrylic adhesive used in cell interconnection components. As the high-concentration cells used for the test receiver are very thin, and soldering them can be difficult and damaging to the cell's performance, the project team used self-adhesive copper tape to provide a solderless electrical

contact between adjacent cells. Apparently, at an elevated temperature and with short circuit currents as high as 2 amps at 40 suns concentration, the acrylic-based adhesive loses its conductive properties, often resulting in the total loss of electrical contact. In order to verify that the PV failures were due to bad electrical contacts, we assembled another receiver based on an array of one-sun space cells and soldered the electrical connections.

Despite its 20% higher operational temperature (due to a small heat sink), the second test receiver performed normally for hours of continuous operation with and without short circuit testing. The current-voltage (I-V) curve obtained for this receiver was stable. In another test, one of the five-cell PV modules remanufactured with soldered contacts also performed without any notable degradation under the full concentration (Figure 20).

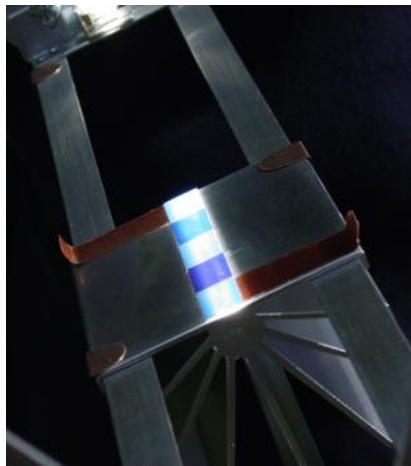


**Figure 20. Remanufactured PV receiver with soldered contacts**

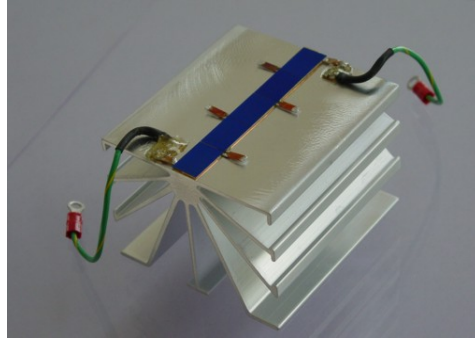
Photo Credit: SVV Technology Innovations

## 2.3 Technical Feasibility Assessment

### 2.3.1 Test Setup

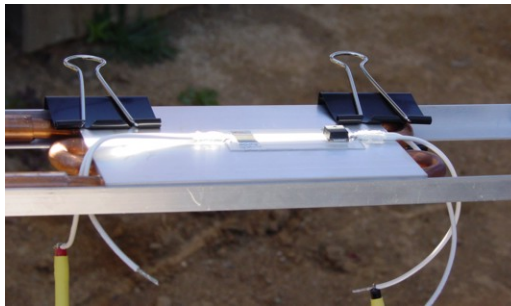
Based on the above experiments, a series of separate but smaller PV receivers were developed to facilitate measurements and reduce the likelihood of individual cell failure during testing. Several PV receiver modules were fabricated for testing the concentrator as a CPV device. One of these receivers is shown in Figure 21.

Another test receiver with referenced characteristics was procured. This receiver is based on a single 30%-efficient triple-junction cell having 1 cm × 1 cm (0.4 in × 0.4 in) active area and mounted on a cooling plate as shown in Figure 22. An active water pumping chiller, shown in Figure 23 was assembled to improve heat dissipation and keep the cell temperature low.



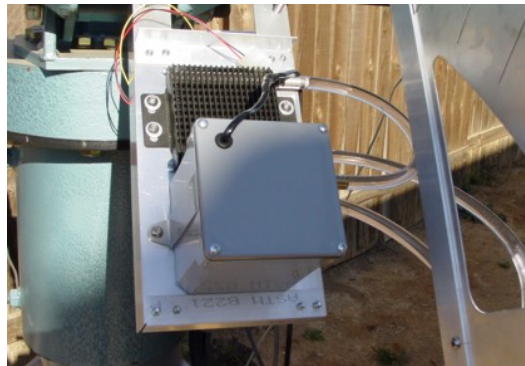
**Figure 21. A new five-cell PV receiver module**

Photo Credit: SVV Technology Innovations



**Figure 22. A single-cell reference PV module**

Photo Credit: SVV Technology Innovations



**Figure 23. A water-carrying chiller for the reference PV receiver**

Photo Credit: SVV Technology Innovations

The test setup included optical and electrical components, each aimed at independently verifying the concentrator efficiency and optical performance. The optical portion was based on digital CCD imaging, with the concentrated flux visualized by a uniformly scattering target. Light profiles of the captured digital images were used for tracing the energy distribution across the focal line, and estimating the amount of light that reached the target after being reflected from the concentrator. The electrical testing was based on measuring the current and power output of various PV receivers placed in the concentrator's focus, and comparing the results with the corresponding parameters of the same receivers exposed to the ambient (non-concentrated) sunlight. Figure 24 shows different parts of the test setup.

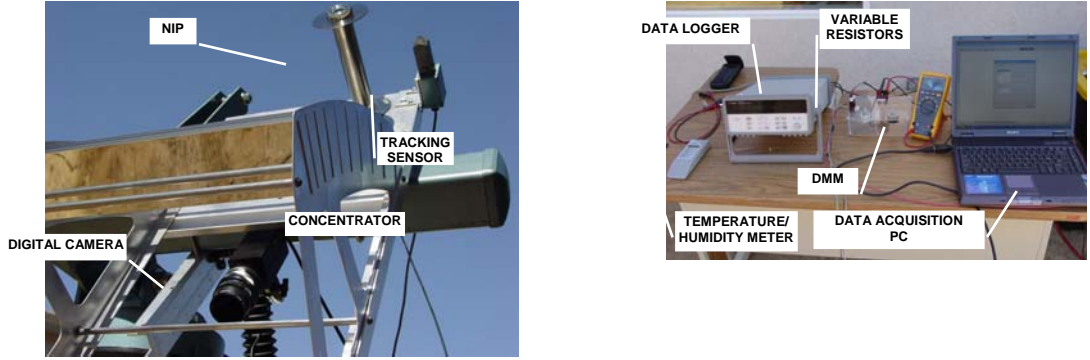


**Figure 24. Concentrator test equipment**

Photo Credit: SVV Technology Innovations

### 2.3.2 Methodology and Testing Procedures

#### Electrical and Power Output Measurements

The geometrical concentration ratio  $C_G$  of an optical sunlight collector can be estimated from the ratio of corresponding levels of direct solar irradiance for the same receiver area exposed to concentrated and non-concentrated fluxes ( $F_{D \text{ concentrated}}$  and  $F_D$ , respectively):

$$C_G = \frac{1}{\eta_{opt}} \cdot \frac{F_{D \text{ concentrated}}}{F_D}, \quad (4)$$

where  $\eta_{opt}$  is the optical efficiency of concentrator.

On the other hand, the short circuit current generated by a monocrystalline-silicon concentrator cell is proportional to the level of irradiance:

$$I_{sc} = k_T \cdot \eta_{cell} \cdot F_G, \quad (5)$$

Where  $I_{sc}$  is the short circuit current of the cell at a certain global solar irradiance level  $F_G$ ,  $\eta_{cell}$  is solar to electric conversion efficiency of the cell and  $k_T$  is a temperature coefficient for  $I_{sc}$ .

Accordingly, concentrated short circuit current  $I_{sc \text{ concentrated}}$  for the same cell exposed to the concentrated flux at the same global irradiance level:

$$I_{sc \text{ concentrated}} = k_T k_{\Delta\theta} \cdot \eta_{cell} \cdot F_{D \text{ concentrated}}, \quad (6)$$

where  $k_{\Delta\theta}$  reflects the optical effects of off-normal incidence angles  $\theta$ .

As the short circuit current of silicon concentrator cells depends little on temperature in the range of 20°C to 70°C ( $k_T \approx 1$ ), obtain

$$I_{sc} \approx \eta_{cell} \cdot F_G \quad \text{and} \quad I_{sc \text{ concentrated}} \approx k_{\Delta\theta} \cdot \eta_{cell} \cdot F_{D \text{ concentrated}}. \quad (7)$$

Now obtain from (4) and (7):

$$C_G \approx \frac{1}{\eta_{opt} k_{\Delta\theta} F_D / F_G} \cdot \frac{I_{sc \text{ concentrated}}}{I_{sc}} \quad (8)$$

Accordingly, the concentrator optical efficiency can be found from the following expression:

$$\eta_{opt} \approx \frac{1}{k_{\Delta\theta} C_G F_D / F_G} \cdot \frac{I_{sc \text{ concentrated}}}{I_{sc}} \quad (9)$$

Now, using (3) and (9) obtain for optical efficiency:

$$\eta_{opt} \approx \frac{A_R}{A_C} \cdot \frac{F_G}{F_D} \cdot \frac{1}{k_{\Delta\theta}} \cdot \frac{I_{sc \text{ concentrated}}}{I_{sc}} \quad (10)$$

Each concentrator cell used in the prototype has the width of 1 cm (0.4 in). The corresponding width of the prototype concentrator is about 38 cm (15 in) making the ratio of concentrator and receiver apertures of about 38 ( $A_C / A_R = 38$ ).

Taking into account the current geometry of the prototype SAC ( $0 \leq \theta \leq 34^\circ$ ) and literature reported dependences of  $I_{sc}$  from the incidence angle for silicon cells, the optical losses due to the off-normal incidence are estimated to be around 5% ( $k_{\Delta\theta} \approx 0.95$ ).

The direct component of solar irradiance for clear sky conditions at Sacramento's latitude and for relatively small zenith angles of the sun at which most of the measurements were conducted typically constitutes 90 to 95% from global radiation. Thus, assuming it is about 95% of global ( $F_D / F_G = 0.95$ ), obtain:

$$\eta_{opt} \approx 0.029 \cdot \frac{I_{sc \text{ concentrated}}}{I_{sc}} \quad (11)$$

The efficiency of a solar cell or a group of electrically interconnected cells is defined as electrical power out divided by light power  $P_I$  incident to the cell aperture:

$$\eta_{cell} = \frac{V_{mp} I_{mp}}{P_I} \quad (12)$$

where  $I_{mp}$  and  $V_{mp}$  are, respectively, the current and voltage corresponding to a maximum power output of the cell(s) at a given  $P_I$ .

The fill factor FF, being defined as the ratio of the peak power to the product  $I_{sc} \times V_{oc}$ , determines the shape of the solar cell I-V characteristics. Its value is higher than 0.7 for good cells. The series and shunt resistances account for a decrease in the fill factor.

The individual concentrator cells that the project team used are optimized for concentrations of about 100 suns. They are designed to have FF values of about 0.76 at 25 W/cm<sup>2</sup> illumination level and above 0.81 at 9.6 W/cm<sup>2</sup> (100 suns) and below.

Similarly to (12), the total solar to electric efficiency  $\eta_{CPV}$  of a concentrator PV system can be determined from the following expression:

$$\eta_{CPV} = \frac{V_{mp} I_{mp}}{P_{IC}}, \quad (13)$$

where  $P_{IC}$  is the direct incident energy collected by the active concentrator aperture  $A_C$  corresponding to the cumulative receiving aperture of PV cells.

For a CPV with 38 suns geometrical concentration and a receiver consisting of 5 cells, each having an active area of 1.45 cm<sup>2</sup> (0.225 in<sup>2</sup>), we have:  $A_C = 1.45 \text{ cm}^2 \cdot 5 \cdot 38 = 275.5 \text{ cm}^2$  (42.7 in<sup>2</sup>). Thus, at the direct normal irradiance of 1,000 W/m<sup>2</sup>, we have:  $P_{IC} = 275.5 \text{ W}$ .

The short circuit current relationships and I-V curves of selected PV receivers were traced by measuring the direct current  $I_{DC}$  and  $V_{DC}$  values at different circuit loads controlled with a series of variable resistors. Each I-V pair of measurements was time stamped and complemented with simultaneous recordings of cell temperature and direct solar irradiance. The successful series of measurements were accompanied by reading and recording the ambient conditions and other relevant information.

A normal incidence pyrheliometer (NIP) from Eppley Lab was used for measuring the level of direct solar irradiance. It was installed on the same tracking platform as the concentrator and a directional sunlight sensor to ensure correct measurements at all times when the concentrator was pointed at the sun. Relative humidity and ambient air temperature were measured with a Vaisala HM34 humidity and temperature meter. The cell temperature was measured with a J-type thermocouple, having the accuracy of 1°C. The sensitive end of the thermocouple was attached to one of the copper electrical contacts of PV cells close to the cell's edge.

A data acquisition/data logging unit (see Figure 24) was used for I-V curve tracing. It was equipped with an HP-34901A 20-channel Multiplexer and set up to record multiple input signals including  $I_{DC}$ ,  $V_{DC}$ , cell temperature, and the level of direct incident solar radiation on different channels. A Fluke-179 DMM was used to independently check and measure the  $V_{oc}$  and  $I_{sc}$  parameters of the circuit.

The NIP channel of the data logger was configured to record and display the direct irradiation in W/m<sup>2</sup> units, according to the factory-provided device sensitivity, and using the scaling functions of the unit. The input on  $I_{DC}$  channel, with a measurement limit of 1A, was conditioned with a

low-ohmage shunt of a known resistance to extend the measurement range to several Amps. The voltage and temperature did not require any conversion and were measured by the internal DMM and recorded by the data logger directly.

Each data scan was initiated manually from the control software on the front panel of the unit, and included automatic readings of all four parameters, with 6½ multimeter accuracy in less than 0.1 second. The measured parameters were time-stamped and recorded simultaneously to the data logger’s internal memory.

A complete I-V curve was recorded as a sequential set of individual scans taken at two to five second intervals for incremental values of circuit resistive load. It took, on average, 30 to 50 data points and one to two minutes to trace each individual curve.

The data logging unit was configured for measurements with control software from HP (Figure 25) using the RS-232 interface. The same software was also used to upload the successful scans to a laptop PC for on-the-fly reviewing and for storage and processing.

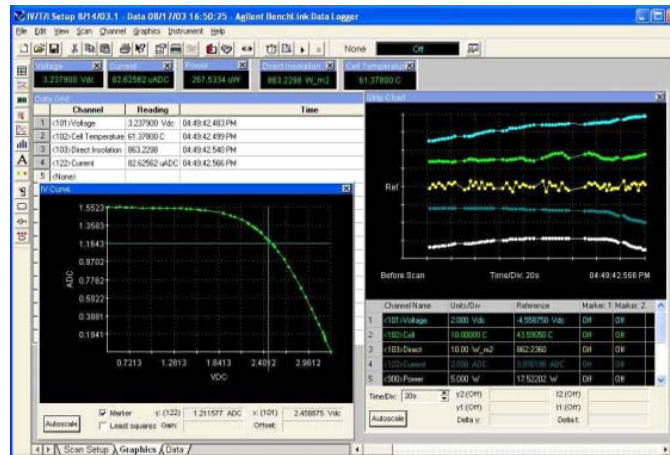


**Figure 25. A screenshot of data acquisition and control software.**

**Photo Credit: SVV Technology Innovations Optical Measurements**

The project team used a monochrome CCD camera, the CFW-1310M from Scion Corp., to capture digital images of the focal spot, with a spatial resolution of 1360 × 1024 pixels and 10-bit dynamic range.

The digital camera was installed on the tracker’s torque tube at a distance of about 1 ft from the concentrator focal line, and pointed to a focal spot visualized with a light scattering target. The target was a thin glass plate with a layer of compacted barium sulphate powder deposited on one side, facing the concentrator and camera. This type of surface is a good approximation of the ideal Lambertian surface, isotropically scattering the incident light. Its visible brightness depends linearly on the illumination level in a wide range of orientations. A 1 cm (0.4 in) reference scale was attached to the target support plate to assist in measuring the size of the focal spot.

The camera was attached to a data acquisition laptop PC via an IEEE 1394 interface so that the live video bit stream was fed directly to the computer and captured by the “Scion Capture”

control software provided by the camera manufacturer. The camera settings, as well as appropriate exposure and gain, were selected through the software. The research team used the highest brightness values for the image pixels to select the gain and utilize the maximum dynamic range of the CCD camera.

The camera optics were based on the Helios-44 lens, having a 58-mm focal length and a built-in variable diaphragm. The focus of the camera was set manually, using lens adjustment rings and visual monitoring of image sharpness on the computer screen. A set of neutral density optical filters was used to control the amount of light entering the CCD and prevent its overexposure.

Focal images were captured as individual frames of the live video stream using the standard software interface to the camera. The images were encoded in a lossless TIFF format and stored on the computer hard drive for processing.

A complete set of images for each exposure included: pictures of the concentrator-illuminated target; a series of pictures capturing the irradiance background on the target, with and without direct sunlight illumination; a one-sun illuminated target (two and three suns when appropriate); and a closed-diaphragm background (the dark current of the CCD). The one-sun illumination level was measured by exposing the target to the direct normal solar radiation. An alternative method for estimating the one-sun irradiance level was achieved using flat mirrors laminated with a silvered, 95%-reflective film, and positioned to reflect the sunlight to the target.

The brightness of a Lambertian surface is proportional to the level of surface irradiance in a wide range of viewing angles, and in a broad light spectrum. In turn, the light signal coming from the plate surface and recorded by a CCD as electron-counts per pixel  $N_e$ , is proportional to the apparent surface brightness. The digital CCD camera converts the accumulated electron-counts into voltage, and outputs the recorded signal in the form of a bitmap image, representing a two-dimensional array of numbers (counts)  $N_c$  encoded as pixel gray values. Its conversion from units of electron-counts to counts can be simply expressed using the camera gain  $G$ :

$$N_c = \frac{1}{G} N_e \quad (14)$$

The scientific-grade cameras are fundamentally linear, offering a high signal to noise ratio in bright field conditions (small  $G$  values). Thus, the number of signal counts (gray level) recorded in each pixel of the output still image is linearly proportional to the corresponding level of target surface illumination by a concentrated flux:

$$N_c = k_c \cdot F_G, \quad (15)$$

where  $k_c$  is the gray level to surface irradiance conversion factor.

The conversion factor  $k_c$  depends on camera optics, incident flux attenuation with neutral density filters, distance from camera to the surface, and camera gain. However, if these parameters are kept constant, the useful signal level  $N_c$  depends on the surface illumination

only. Therefore, the actual concentration  $C_A$  for each pixel of the output image can be estimated from the ratio of  $N_C$  to the signal level  $N_{C-1SUN}$  corresponding to one sun illumination  $F_{G-1SUN}$ :

$$C_A[suns] = \frac{F_G}{F_{G-1SUN}} = \frac{N_C}{N_{C-1SUN}} \quad (16)$$

### 2.3.3 Findings and Analysis

#### Power Output

Table 2 shows the peak values of  $I_{sc}$  and  $I_{sc\ concentrated}$  measured at normal operating temperatures for different test receivers during August through September, 2003. All measurements were normalized for 1,000 W/m<sup>2</sup> direct incident power. The table also shows the corresponding values of concentrator's optical efficiency calculated according to formula (11) and expressed in percentages.

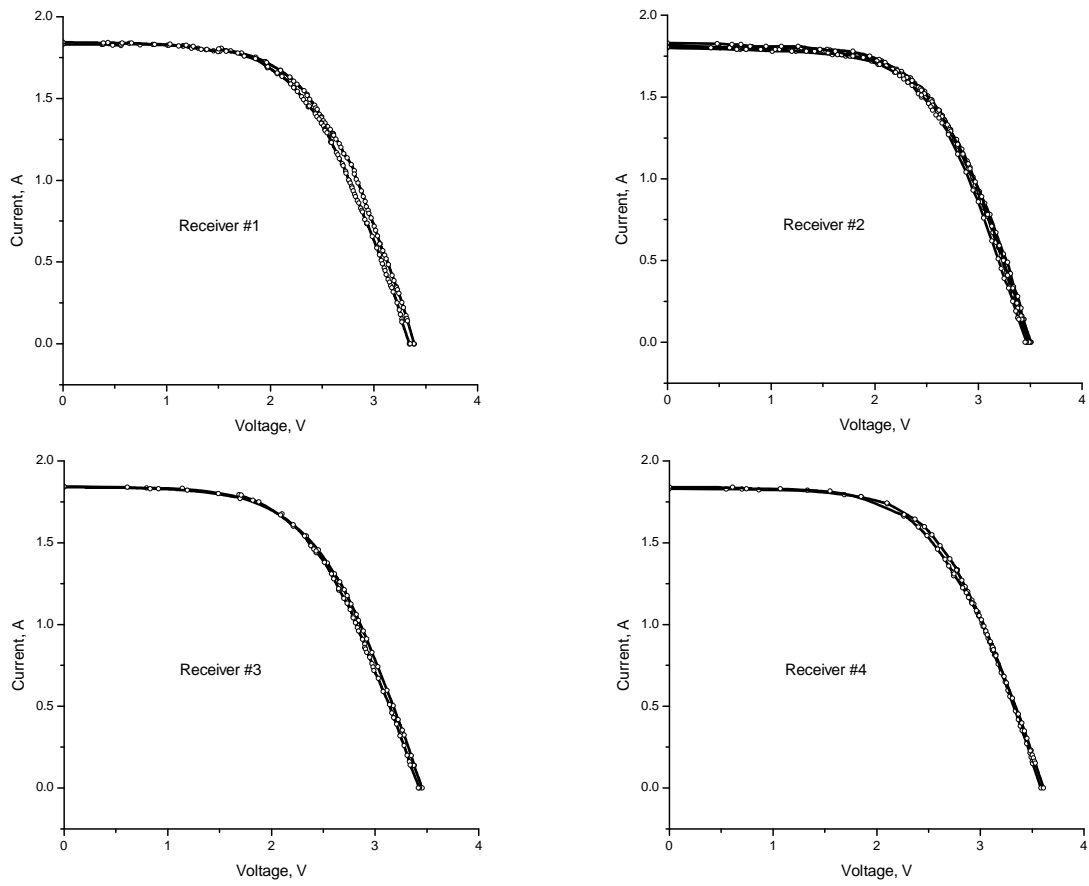
**Table 2. Concentrator optical efficiency estimated from  $I_{sc}$  measurements.**

Receiver	$I_{sc}$ , mA	$I_{sc\ concentrated}$ , A	$\eta_{opt}$ , %
#1	0.063	1.845	84.9
#2	0.062	1.830	85.6
#3	0.064	1.845	83.6
#4	0.063	1.840	84.7

Source: Data collected by Sergey Vasylyev

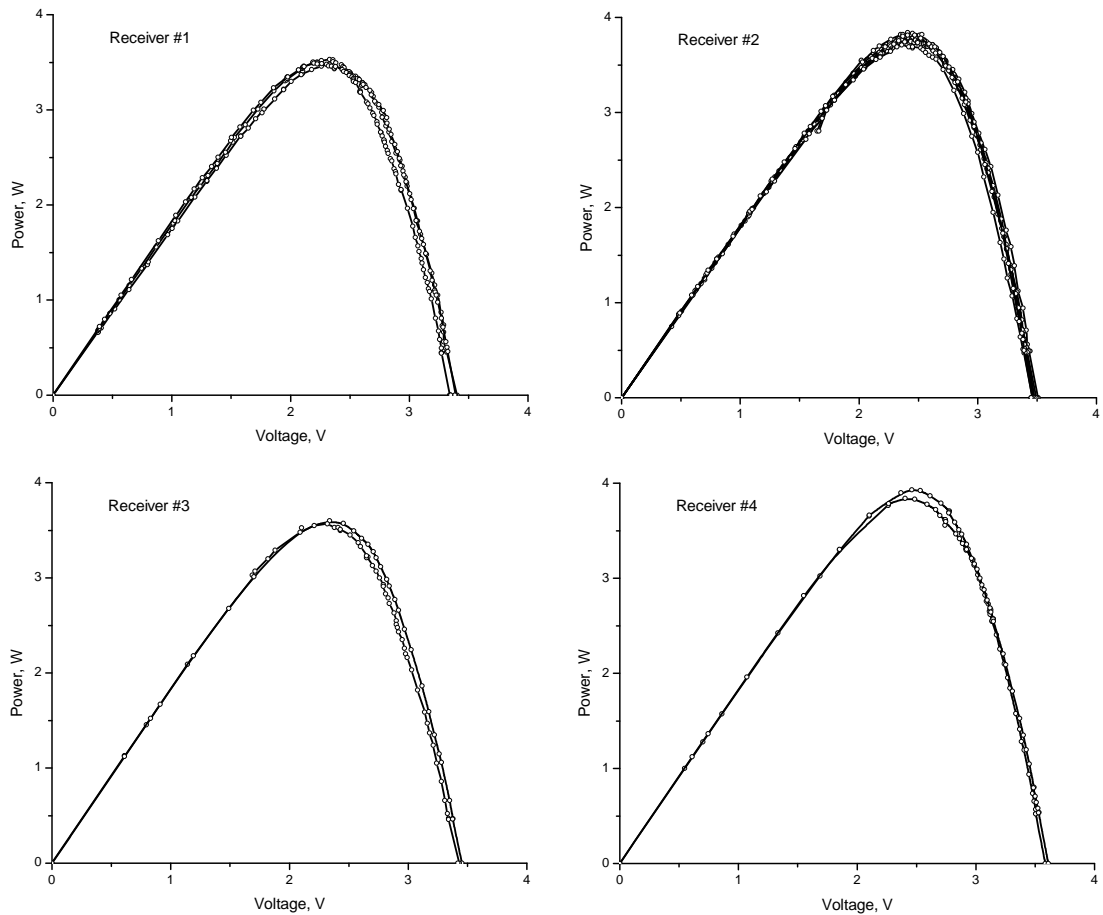
The estimated optical efficiencies shown in Table 2 vary only slightly, from 83.6% to 85.6%, thus exhibiting good consistency for different receivers and sunlight conditions. The experimental data also correspond with the predicted concentrator efficiency for the small prototype (85%). Note that the predicted efficiency was based on the ideal mirror reflectivity of 95%, while the factory-measured maximum reflectivity of Alanod aluminum used for the prototype is only 92%. This confirms the high performance of the slat-array optics.

Figure 26 shows normalized I-V curves obtained for different receivers, and Figure 27 shows the corresponding power curves. Each data point was normalized to 1000 W/m<sup>2</sup> direct irradiance. The curves obtained are quite representative for the respective receiver modules, exhibiting negligible differences in both current and voltage, resulting in a relatively stable maximum power output.



**Figure 26. I-V curves measured for four different CPV**

Photo Credit: SVV Technology Innovations



**Figure 27. Power curves for the same PV receivers shown in Figure 26**

Photo Credit: SVV Technology Innovations

Figure 28 shows some selected I-V curves for different receivers plotted on the same graph. The corresponding P-V curves are shown in Figure 29. Despite the fact that the data were obtained at different dates and zenith angles of the sun, the behavior of electrical current is consistent for all receivers, indicating similar normalized illumination levels for the cells.

While showing a 3 to 4% difference between the receivers, the absolute magnitude of  $V_{oc}$  and its variation were within the anticipated range. The research has shown that, for crystalline silicon cells, voltage decreases with an increase in cell temperature by approximately 0.45% per degree C, or 4.5% decrease at 10°C (50°F). According to the spec sheet for the concentrator cells, their temperature coefficient for  $V_{oc}$  was about 0.22% per degree, which corresponds to a 2.2% drop in voltage at a temperature increase of 10°C. The average cell operating temperatures ranged from about 55°C to 65°C (131°F to 149°F) for the selected measurements, where the differences in individual measurements between the receivers were 15°C (59°F) and above.

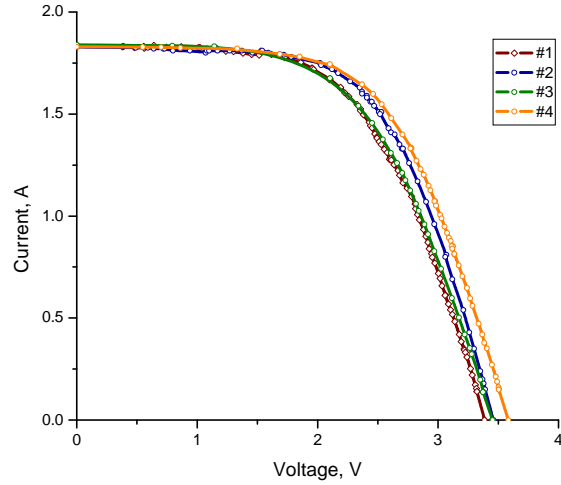


**Figure 28. Selected I-V curves for different receiver modules**

Photo Credit: SVV Technology Innovations

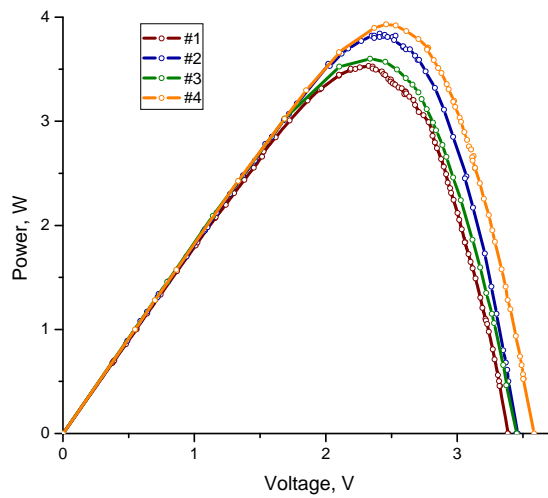


**Figure 29. Power curve comparison**

Photo Credit: SVV Technology Innovations

Thus, the electrical measurements of  $I_{sc}$  and  $V_{oc}$  parameters of I-V curves, being consistent for different receivers and sunlight conditions, and falling into the range of anticipated values, confirm the high optical performance of initial prototype CPV and the SAC.

The total power output from test receivers under the variable resistive load was somewhat below expectations. It indicated that the overall solar to electric efficiency of the system was affected by some imperfections in the PV receiver design.

The measured FF values obtained for the test receivers containing five series-connected cells were well below expectations at about 0.69-0.7 for one-sun flux, and about 0.60 for 40 suns concentrated flux. Both values were based on the characteristics of a single cell. The reason for such degradation of the fill factor could be a mismatch in series resistance of the cells within each five-cell module, insufficient thermal conductivity of cell/heat-sink interface, and even partial damage of the extremely fragile cells during soldering at the time of receiver fabrication.

The peak power output by #4 test receiver was 3.93 W at  $I_{mp} = 1.60$  A and  $V_{mp} = 2.46$  V.

Therefore, the resulting peak efficiency  $\eta_{CPV} = 3.93/27.55 = 14.3\%$ .

The obtained specific efficiency of the prototype system using the 40 suns concentrator and 22%-efficient cells was lower than we expected (16 to 18%), which appears to be mainly due to the effect of reduced fill factor. Nevertheless, it still compares well to the efficiencies obtained from other CPV studies involving 18 to 20% efficient cells, and typically reported to be between 10% and 14%.

Figures 30 and 31 show the measured I-V and power curves for the reference receiver from Spectrolab. As evidenced by the plotted data being normalized to 1kW/m<sup>2</sup> direct irradiance level, the factory-manufactured receiver performed significantly better than any of the receivers fabricated in-house using SunPower cells. Different measurements conducted at different times produced very similar results. The cell temperature was kept nearly constant, at about 25°C, to simulate normal test conditions.

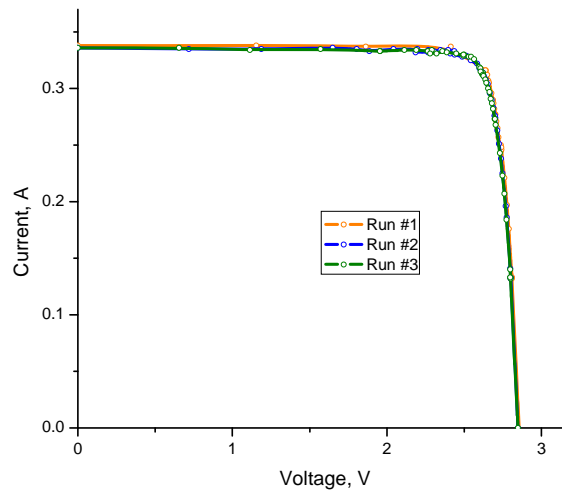


**Figure 30. Experimental I-V curves for the reference receiver**

Photo Credit: SVV Technology Innovations

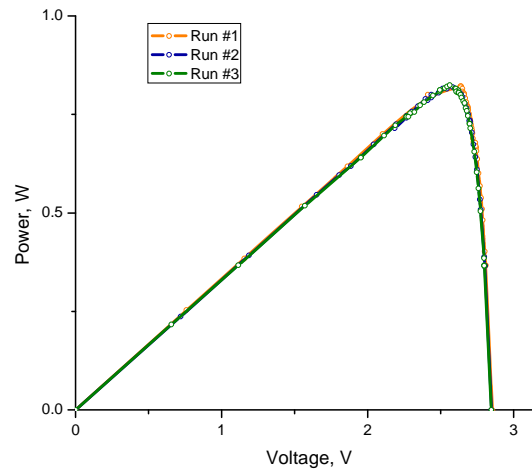


**Figure 31. Power curves for the reference receiver**

Photo Credit: SVV Technology Innovations

Table 3 shows the comparison of CPV-measured electrical parameters with the corresponding data for a triple-junction cell. The reference data was obtained by interpolating corresponding cell characteristics for  $V_{oc}$ , FF and  $\eta_{cell}$  at different concentration levels available from the manufacturer.

**Table 3. Comparing measured and reference cell parameters.**

Parameter	CPV module (prototype)	Reference cell (30-40 suns)
$I_{sc}$ , A	0.34	N/A
$V_{oc}$ , V	2.85	2.83
FF	0.87	0.87-0.88
Max power, W	0.84	N/A
$\eta_{CPV} (\eta_{cell})$ , %	22.0	28

Source: Data collected by Sergey Vasylyev

The measured  $V_{oc}$  and FF parameters are very close to those provided by the manufacturer and based on solar simulator measurements at NREL. The total solar to electrical efficiency of the prototype CPV calculated using (13) is 22%, 78.6% of the rated efficiency for the cell.

Assuming that the electrical efficiency of the reference cell is the same as rated peak efficiency (28%), the total optical efficiency of the prototype CPV system is nearly 80%. The cell can be responsible for a significant amount of optical loss, due to the presence of off-normal incident rays and possible mismatch between the cell spectral response and the spectrum of concentrated beam. The optical efficiency of the concentrator is estimated to be about 85%, which is the same as the efficiency estimated with the in-house fabricated receivers.

## Flux Maps

Figure 32 shows a sample focal image and corresponding relative flux distribution in the concentrator focus, where the concentration level was calculated after subtracting the background and dark current noise from the corresponding  $N_C$  and  $N_{C-1SUN}$  values. The scale in photograph on the left is graduated in one mm increments.

The analysis of irradiance distribution and plotted flux map confirms that more than 95% of the direct solar radiation collected by the prototype SAC is confined within the boundaries corresponding to a 1 cm (0.4 in) wide receiver, thus confirming the validity of the project team's geometrical concentration ratio estimates of 38 suns, based on ray tracing. It also confirms that the selected concentrator fabrication technique was adequate, in terms of manufacturing tolerances for providing the desired performance.

As Figure 32 illustrates, the irradiance of central zones of the receiver does not exceed 60 suns for almost an average 40 suns geometrical concentration. This means the hot spot in the receiver center has been substantially reduced in relationship to other concentration methods. Despite the fact that the actual energy profile is not shaped exactly the same as the calculated one, notable flattening of the central part of measured distribution can clearly be seen.

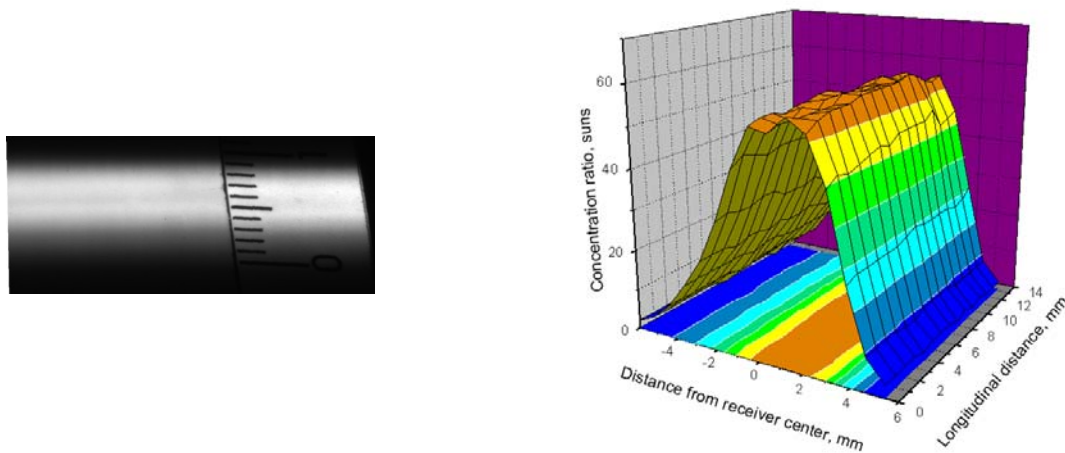


**Figure 32. Focal image and measured irradiance distribution in the focal spot**

Photo Credit: SVV Technology Innovations

The geometrical concentration revealed good stability with respect to receiver misalignment or small displacements, as well as concentrator tracking errors of up to  $0.3^\circ$ . As expected from ray tracing, large longitudinal misalignments of up to  $45^\circ$  (larger angles were limited by the current prototype design), simulating one-axis tracking, showed only the effects of cosine dependence of surface illumination on the incident angle.

However, the uniformity exhibited a considerable sensitivity to the proper receiver positioning and alignment. The replacement of individual slats and the effects of slats being slightly loose in

the side wall slots also affected the shape of flux distribution without degrading the overall concentration.

Figure 33 shows the change in flux map for a receiver which is moved away by two to three millimeters from the designed focus. It can be noted that, despite the fact that the flux distribution became sharper, exhibiting a higher concentration in the receiver center, the “flat” area degraded significantly. Nevertheless, the peak concentration increased by only 10 to 15%, still well below the 100 suns which could be expected in a traditional system designed for 40 suns geometrical concentration, with no provisions for uniformity.

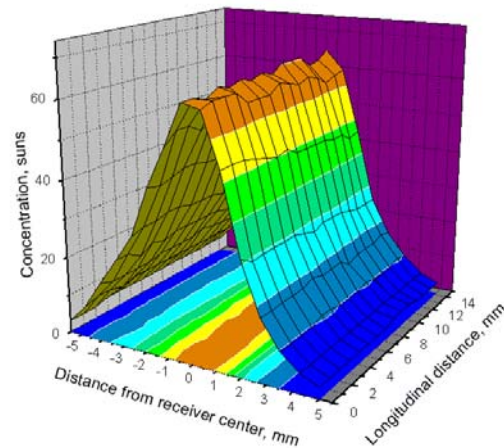
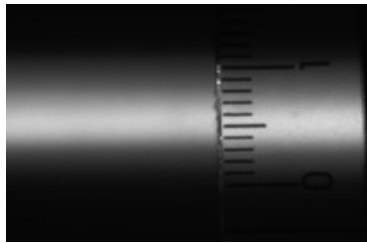


**Figure 33. Irradiance distribution for a displaced receiver**

Photo Credit: SVV Technology Innovations

### ***Reflector Weight and Material Costs***

The reflector of the prototype SAC with was fabricated using 10 strips of solar-grade aluminum, each having the dimensions of 425 mm × 80 mm × 0.5 mm (17 in × 3.1 in × 0.02 in), and weighing about 47 grams (1.5 oz). The reflector weight is therefore 0.470 kilograms (1.26 lbs), which makes the weight to active aperture ratio of less than 3 kg/m<sup>2</sup> (0.75 lbs/ft<sup>2</sup>), considering the active area of the initial prototype SAC of 0.16 m<sup>2</sup> (about 1.7 ft<sup>2</sup>). This is probably the most lightweight reflector ever used for such a high concentration.

Adding the slat reinforcement ribs, made from aluminum coil and weighing about 20 grams each, brings the total weight of the reinforced reflector to about 4.2 kg/m<sup>2</sup> (1 lbs/ft<sup>2</sup>), which is about the same as the weight of a bare 6061 aluminum sheet of the same area, with 1.6 mm (0.063 in) thickness. This is still considerably less than the reflector weight of simple parabolic troughs.

The cost of reflective aluminum used for slats was about \$20 per m<sup>2</sup>. As the SAC consumes about 2 square meters of reflective laminate per square meter of aperture, a non-reinforced reflector would be about \$40/m<sup>2</sup>. The coil rib reinforcement adds an extra \$10/m<sup>2</sup> to the reflector cost (considering the retail price, current consumption of aluminum coil, and adhesive transfer tape in

the prototype). However, this reinforcement system significantly offsets the cost of reflector support, since no extra arrangement for maintaining the slat shapes is needed.

The rigid frame of the small CPV prototype, which supports the mirror and PV receiver, weighs less than a kilogram, or about 6 kg/m<sup>2</sup> (1.5 lbs/ft<sup>2</sup>). It weighs much less than the support frames of traditional concentrators for the same area. Moreover, these calculations were made based on the current prototype design, with a 43 cm (17 in) slat length. In a commercial system, the authors expect this length to be 0.91 to 2.74 m (3 to 9 ft), which will further reduce the specific weight per unit aperture.

## **2.4 Design of a Commercial-Size Prototype**

The results of testing the initial small prototype were analyzed to develop recommendations for improving the slat-array PV concentrator design. Design considerations for the scaled-up prototype included the concentrator adaptation for lower-concentration PV cells, improvement in the optical scheme, and optimization of the structure.

A number of changes/improvements to the design were made, improving upon the initial small prototype. The improved SAC consists of two identical parts facing each other and forming a very low profile, symmetric configuration. The ASCEND computer program was updated to support the symmetric modular arrangements of the improved SAC.

### **2.4.1 Design Improvement**

The SAC design was adapted to a larger size of 2.79 m<sup>2</sup> (30 ft<sup>2</sup>) and its geometry and structure were improved. The concentration ratio was reduced to 20 suns to target a broader range of existing and future concentrator PV cells, and possibly even high-quality one-sun cells that accept low levels of concentration. The new symmetric arrangement allowed the research team to fully utilize the concentrator aperture, minimize gaps between modules, and further lower the concentrator profile.

The slats were designed to all be the same size and shape. This was a major improvement over the small prototype, since it allowed the project team to make the manufacturing process uniform. Additionally, the slats were almost flat, to reduce the effect of shape imperfections on the concentrator performance. The longitudinal slat stiffeners were also designed to be the same shape and size, to simplify slat fabrication. The dimensions of the stiffeners were calculated with ray tracing, in order to maximize their size and still prevent radiation blocking both for the incident and concentrated solar fluxes.

The new concentrator design included 28 11.7 cm (4.6 in)-wide, 1.83 m (6 ft) long reflective slats incorporated in two symmetrical segments, each focusing the incident sunlight onto a respective focal line. It was optimized for a 4 cm (1.57 in) wide PV array that is uniformly illuminated.

### **2.4.2 New Optical Configuration**

The project team investigated the possible use of secondary reflectors with the final prototype. The ray tracing experiments have shown that the use of simple secondary reflectors can help minimize the PV cell area and further improve flux uniformity. The secondary reflectors are merely a pair of narrow reflective strips, designed to increase the concentrator's sunlight

collection ability by 4 to 5%, and homogenize the concentrated flux without impairing the system optical efficiency. As a result, the optical tolerances of the concentrator to shape and alignment errors have also been improved.

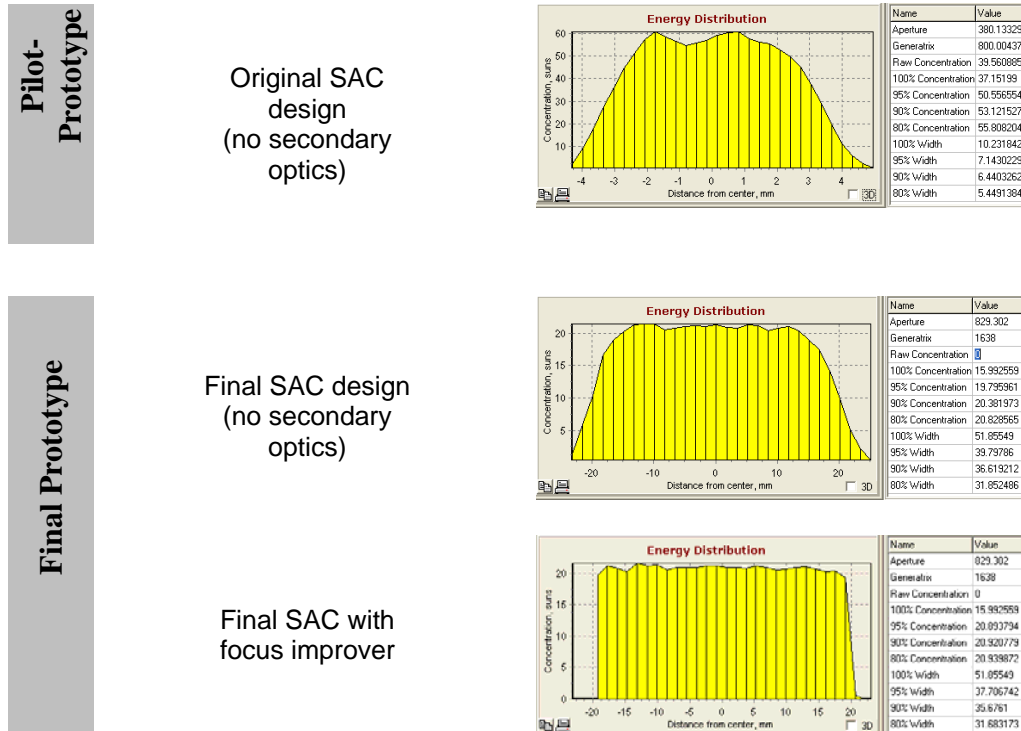


**Figure 34. Irradiance distribution comparison**

Photo Credit: SVV Technology Innovations

Figure 34 compares the calculated energy distributions for the final prototype and the first (small) prototype. These cross-sectional irradiance distribution plots were obtained with the latest version of ASCEND software.

## 2.5 Fabrication of 30 ft<sup>2</sup> Prototype

### 2.5.1 Design and Fabrication of SAC Frame

The frame fabrication included designing and manufacturing precise cross-sectional templates, replicating the optical configuration of the target concentrator prototype. This approach allowed the research team to eliminate the laser cut sidewalls from the SAC design, and replace them with simpler, more lightweight components. The templates were computer aided design (CAD) drawings, based on the data generated by the ASCEND software, used for precise laser cutting. Figure 35 shows the finished templates cut by a local sheet metal fabrication shop.



**Figure 35. Laser cut aluminum templates.**

Photo Credit: SVV Technology Innovations

The narrow curved slots seen in the Figure 35 are designed to fit 0.1524 cm (0.06 in) thick inserts fabricated from an aluminum angle bent to the radius corresponding to the slat curvature. The concentrator slats were securely mounted to the inserts to ensure their proper alignment and to add structural rigidity to the system.

The improved and final SAC prototype frame (Figure 36) was designed to accommodate two symmetrical arrays of 6-foot reflective slats, as well as two PV receivers mounted underneath the concentrator. As a result of experiments with different arrangements and frame simplification, the frame was constructed using only widely available and low-cost raw stock materials, such as aluminum angles and square tubing, while maintaining the tolerances required for proper optical functionality. All frame components were designed to be either straight or bent to a constant radius with a simple bench top tool. The curvature radius of the manufactured parts was controlled with a digital arc meter and a set of precisely cut arc templates.

Figure 36 shows the experimental frame fabricated with the use of laser-cut templates. Besides being much larger than the experimental frame of the small pilot prototype, the new frame provides a number of improvements over the previous design.



**Figure 36. Improved Support Frame for 30- ft<sup>2</sup> Concentrator**

Photo Credit: SVV Technology Innovations

### ***2.5.2 Design and Fabrication of Test PV Receiver***

The research team designed and fabricated a test receiver for the 2.79 m<sup>2</sup> (30 ft<sup>2</sup>) concentrator prototype. The receiver was based on a custom concentrator PV kit using high-efficiency triple junction cells. The new receiver design incorporated four series connected cells, densely packed across a 4 cm (1.6 in) wide focal line, and designed to be totally illuminated by the concentrator. Figure 37 shows the receiver design layout. Each cell is 1 cm × 1 cm (0.4 in × 0.4 in). Bypass diodes are included to protect individual PV cells from reverse bias, such as during partial shadowing.

In order to facilitate final prototype testing, the project team decided to combine the electrical (PV) and optical test targets into a single receiver design. As the receiver's cooling plate provides a flat surface with adequate heat dissipation, the team decided to mount an optical target for flux mapping onto the same plate which supports concentrator cells. Similarly to the approach used for the small prototype evaluation, the project employed a retro-reflection light scattering target, allowing quality optical measurements using digital imaging.

Figure 37 also shows a pair of relatively narrow wings of a focus improver, whose optical design was developed in previous tasks. The focus improver is optional, and is used for illuminating PV cells with a 20 suns concentrated beam. This improves the flux uniformity at the edges of the outermost cells.

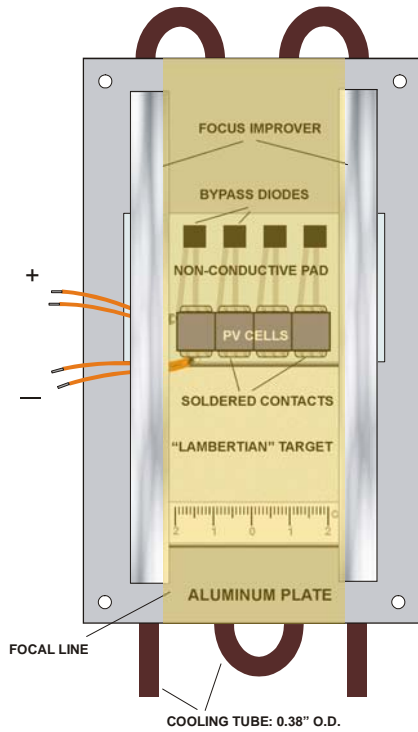


**Figure 37. A scheme of the new four-cells PV receiver**  
 Photo Credit: SVV Technology Innovations

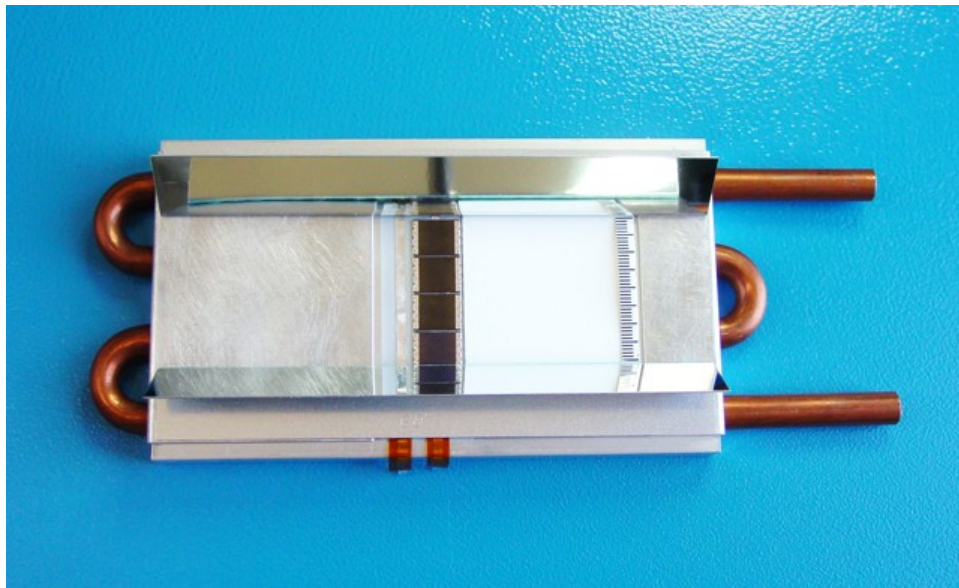


**Figure 38. Test receiver for the final prototype**  
 Photo Credit: SVV Technology Innovations

Figure 38 shows the completed electro-optical test receiver based on the triple junction PV cells. The bypass diodes are not visible, since they were removed from the face of the cooling plate and embedded into the cell assembly. The focus improver was made of narrow and planar strips of 0.5-mm (0.02 in) reflective aluminum. The optical target was made of a thin glass plate covered

with an optically dense layer of compacted barium sulphate powder, closely simulating a Lambertian surface.

### **2.5.3 Fabrication of Concentrator Slats**

As with the first prototype, the concentrator slats were fabricated from 0.5-mm (0.02 in) reflective material (Figure 39) and laminated with a protective plastic film.



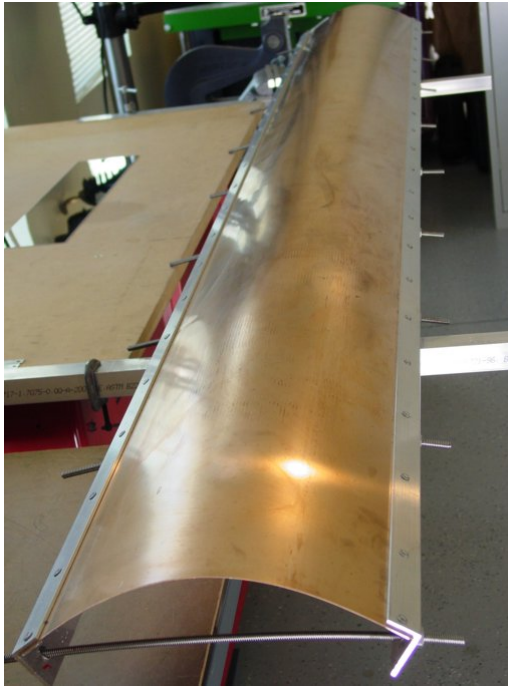
**Figure 39. Raw sheets of reflective material**

Photo Credit: SVV Technology Innovations

The raw sheets were cut into 11.7 cm (4.6 in) wide strips which were bent to a cylindrical radius. The lowered tolerance requirements for this prototype were exploited to test a stretch bend technique for bending the slats to the required cylindrical shape. While slip rolling could still be used for the fabrication of 6 feet long slats for the 2.79 m<sup>2</sup> (30 ft<sup>2</sup>) prototype, as the project team did with the smaller slats, the team used the new technique in order to have greater manual control over the bending process and to be able to fabricate long slats in-house.

An adjustable, stretchable template of about 2.44 m (8 ft) in length was fabricated using a wide strip of phosphorous spring bronze securely clamped between longitudinal support angles, and tensioned using threaded adjustment rods. Figure 40 shows the template. Curvature and tension were experimentally adjusted to consistently produce slats of the required shape. While the transversal profile of the top of the template was not perfectly circular, it was nevertheless close to being circular within the preset allowances. The slat shapes were controlled with laser cut arc templates.

A suitable number of reflective slats were fabricated for the final prototype assembly. The receiver support beams and fixture were also fabricated. A set of slat stiffeners was custom fabricated in a batch operation, using a CNC controlled press brake machine and commercially available aluminum coil. Figure 41 shows a selection of slats prepared for prototype assembling.



**Figure 40. An 8-foot adjustable shape template**

Photo Credit: SVV Technology Innovations

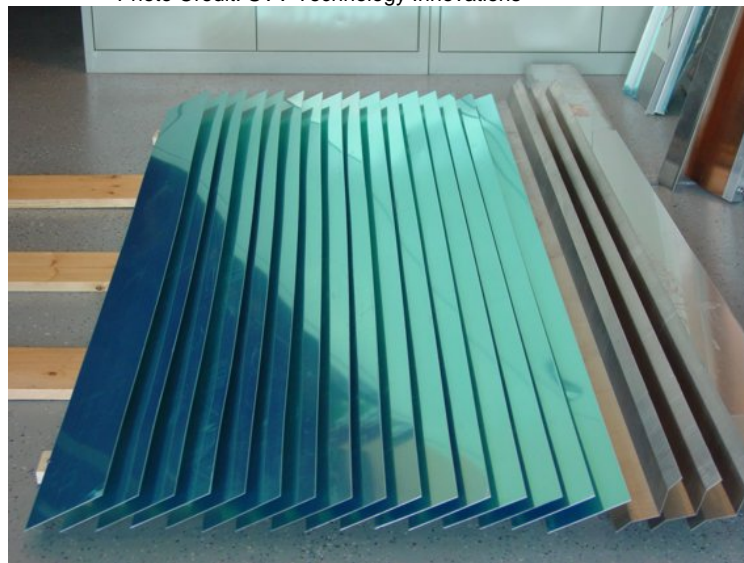


**Figure 41. Cylindrically curved slats fabricated for the final prototype**

Photo Credit: SVV Technology Innovations

The 28 reflective slats were assembled by gluing the stiffeners to the back side of the mirrored strips. A pressure sensitive adhesive tape was used.

In order to facilitate attaching the stiffeners to the back of reflective strips using a high-tackle pressure sensitive adhesive transfer tape, a 1.83 m (6 ft) long stainless steel profile template was also fabricated (see Figure 42). The 12-ga template conformed to the circular shape of the slats and allowed maintenance of the proper slat curvature during assembly operations.

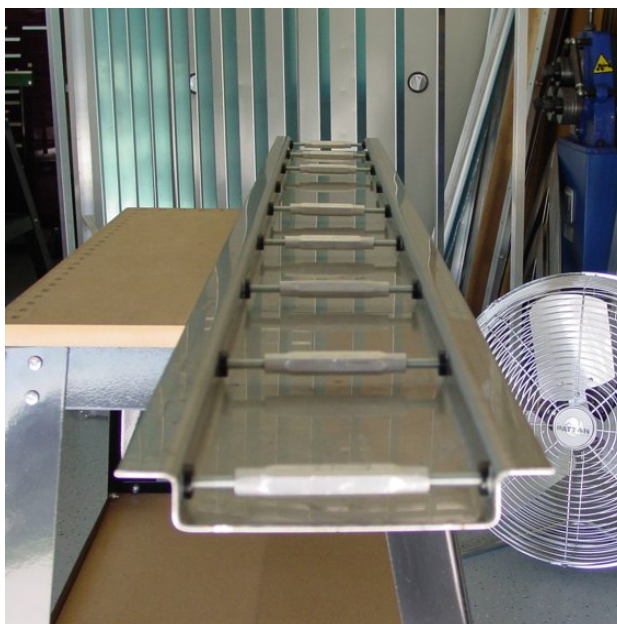


**Figure 42. Tension-adjusted slat shape template**

Photo Credit: SVV Technology Innovations

In addition to the fabrication of the slat-array reflector from Al-anod aluminum, the research team experimented with making slats from a generic aluminum coil laminated with a plastic reflective film. This technique was an improvement, compared to the one the team tested for the small pilot-prototype. The project team laminated sheet material, cut it into strips, and slip rolled each strip to the required shape.

The authors took advantage of the reduced shape tolerances and the flatness of the slats to better preserve the reflective layer, by bending the slats to a concave shape before the lamination, without impairing their optical properties. They were able to use a commercially available bench-top laminator to apply a solar-grade reflective film to the bent slats (see Figure 43). The team observed no notable degradation in the shape of slats after their lamination. This is a promising method for slat reflector fabrication on a larger scale, using a broader variety of inexpensive materials. Although using less expensive materials is more economically attractive, the vendor-provided reflective aluminum remained the material of choice for the final concentrator prototype, mainly due to its good mechanical properties and commercial availability in quantities suitable to support future demand.

Other fabrication methods such as roll forming were also explored for reflective slat and stiffener fabrication. Preliminary profile blueprints were developed and cost and tolerance estimates have been made. The research team concluded that roll forming could be a very attractive alternative for inexpensive slat fabrication in large quantities, if reduced tolerance requirements are met. However, the team decided not to order the roll-formed parts for the prototype concentrator, mainly due to minimum order and project budget limitations.



**Figure 43. Slat lamination with a reflective film**

Photo Credit: SVV Technology Innovations



**Figure 44. The assembled final prototype in the upright position**

Photo Credit: SVV Technology Innovations

#### ***2.5.4 Assembling the Final Prototype***

The slats were mounted to the SAC frame using rivets. Figures 44 and 45 show the assembled prototype concentrator with and without the protective masking film, respectively. The film was kept on the slats during fabrication to prevent possible surface damage.



**Figure 45. The prototype SAC concentrator without film**

Photo Credit: SVV Technology Innovations

Figure 45 illustrates the portability of the 2.79 m<sup>2</sup> (30 ft<sup>2</sup>) concentrator. The final assembly weighed about 30 kg (80.4 lbs), exhibiting a very low weight to aperture ratio of 10 kg/m<sup>2</sup> (2.5 lb/ft<sup>2</sup>), which may be a record low among CPVs, and which is about the weight of flat-panel PV panels. As the photograph shows, the SAC can be easily handled by two people, and therefore can serve as a prototype for portable CPV modules of up to 500 W power capacity, depending on the type of PV cells used. While the evaluation of the prototype performance is covered later in this report, it is evident that this concentrator could reduce the consumption of PV cells by about 20 times, keeping the size and weight of the system fairly low.

A pair of T-shaped aluminum receiver support beams were fabricated and fit into the frame. This provided a suitable mount support for the test receiver and provided additional structural rigidity to the SAC system. The team covered one of the two support beams with a 2-inch wide, 6-foot long, matte-finish, light scattering target as shown in Figure 46. This was used for visualizing the concentrated flux along the entire focal line. The target was fabricated in-house by depositing a high-temperature ceramic spray paint, which was then heat-treated at 600°F to obtain long-term stability and scratch resistance. The test receiver was mounted onto the other support beam for testing the concentrator as a CPV device.



**Figure 46. The receiver support beam with a light scattering target**

Photo Credit: SVV Technology Innovations

The two-axis tracker used for mounting the small pilot-prototype was upgraded by adding a longer torque tube to support the larger prototype system. The SAC was mounted on the tracker for the subsequent evaluation of the final prototype. Figure 47 shows the finished prototype prepared for outdoor tests.



**Figure 47. The final 30-ft<sup>2</sup> SAC prototype mounted on tracker**

Photo Credit: SVV Technology Innovations

### ***2.5.5 Monitoring and Evaluation of the Final Prototype***

The 2.79 m<sup>2</sup> (30 ft<sup>2</sup>) CPV prototype based on the SAC was monitored for about a two-week period to confirm the design improvements and to demonstrate a potential commercial-size module.

The waste heat from the receiver was dissipated using a chiller, using water actively pumped through a fan-cooled radiator. The chiller was based on the same components used for the small prototype evaluation.

The sunlight sensors and measurement equipment included a directional optical sensor mounted on the Eastern side of the torque tube to keep the concentrator pointing at the sun, as well as a factory-calibrated pyranometer, and a normal incidence pyr heliometer, used for measuring the level of solar irradiance. These devices were installed on a single tracking platform, which was mounted to the tracker and aligned with the concentrator to ensure proper positioning of the system with respect to the incident flux and reliable measurements during tests (see Figure 48).

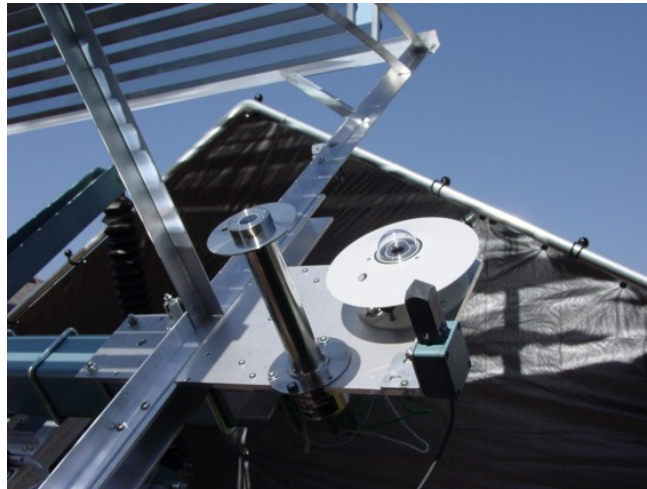


**Figure 48. Solar radiation measurement and tracking sensors**

Photo Credit: SVV Technology Innovations

The DC voltage outputs of the solar radiation meters were fed to separate channels of a signal multiplexer, which were scaled up in accordance with the factory-provided device sensitivity to record and display the irradiation in  $\text{W}/\text{m}^2$  units. This allowed the project team to compare the total and direct solar irradiance levels, and subtract the diffuse radiation to more accurately than previous tests.

A data acquisition/data logging unit was used to capture test data, which also included the short circuit current  $I_{sc}$ , open circuit voltage  $V_{oc}$ , and temperature of the PV cells. The simultaneous multi-channel measurements were uploaded to a laptop PC through an RS-232 interface for further analysis. Relative humidity, ambient air temperature and wind speed were also measured for most sets of I-V measurements.

### ***Sunlight concentration and flux uniformity***

One of the two T-shaped receiver support beams, converted to a 1.83 m (6 ft) long light scattering target, was used to visually assess the quality of the slat-array reflector and concentration ability of the system. The target was painted with a white-color, heat, and radiation resistant ceramic paint cured at a high temperature. Figure 49 shows the focal line projected to the light scattering target, looking outward from inside the final prototype SAC.

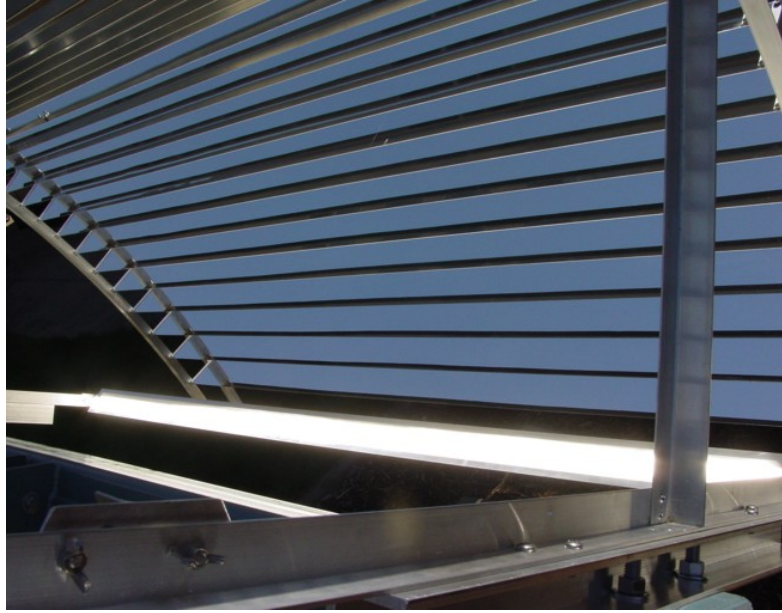


**Figure 49. The concentrator's focal line**

Photo Credit: SVV Technology Innovations

The analysis of the concentrator's focus showed a good correspondence with the designed SAC characteristics and ray tracing. Although the focal line was not absolutely perfect, showing a 10 to 20% difference in its width and flux density along the receiver, these imperfections seem to be reasonable given the greatly reduced manufacturing tolerance for the reflective slats. Despite the bias in the radius of curvature of about 20 to 25% per individual slat, as well as a slight longitudinal bow of some slats that results from the simplified slat fabrication techniques, more than 90% of the concentrated beam was found to be within the designed receiver boundaries. With the focus improver, virtually all incident flux was intercepted. Mirrors used in a parabolic trough would become useless with such slight variations in shape.

The focal spot of the final prototype was estimated to be more uniform than that of the pilot prototype. This was due to the lower concentration ratio of the final prototype, which allowed for the spreading of the concentrated beam across a wider area. The focal line consistently exhibited no unusually hot spots in the receiver center along the focus, which is an advantage for PV. Average flux density of 20 suns might have 22 suns at the highest concentration point. In most conventional concentrators variations in flux density is usually much greater. An average 20 suns conventional concentrator might have 40 suns or even 60 suns at maximum points in the central parts of the receiver.

### ***Optical measurements***

The concentrated flux distribution in the SAC focus was measured using the test receiver and a scientific-grade monochrome CCD camera. The receiver included a small-area (about 25 cm<sup>2</sup> or 3.875 in<sup>2</sup>) Lambertian light-scattering glass target, covered with an optically thick layer of barium sulphate powder. The digital camera captured two-dimensional uncompressed images with a spatial resolution of 1360 × 1024 pixels and dynamic range of 10 bits per pixel.

The camera was mounted to the suntracker using a movable bracket and a flexible arm which allowed the team to capture images of different parts of the focal line from a constant distance of about 0.6 m (2 ft) (Figure 50). Neutral density filters and a variable diaphragm were used to adjust the amount of light entering the camera. The CCD gain was also adjusted programmatically to accommodate the entire range of flux brightness change.



**Figure 50. Digital CCD camera used for capturing focal images**

Photo Credit: SVV Technology Innovations

Figure 51a shows the theoretical energy distribution on the target receiver obtained from ray tracing for this prototype SAC, and Figure 51b shows an actual captured grey-scale image of the focal spot and the corresponding measured flux map.

In Figure 51b the flux map shows some irregularities of the energy profile, apparently due to the imperfections of the concentrator. The overall concentration and shape of the actual irradiance distribution compares well to the profile calculated for an ideal concentrator, and demonstrates that fairly high levels of uniformity can be obtained without secondary optics, using very simple concentrator fabrication technique and reduced manufacturing tolerances.

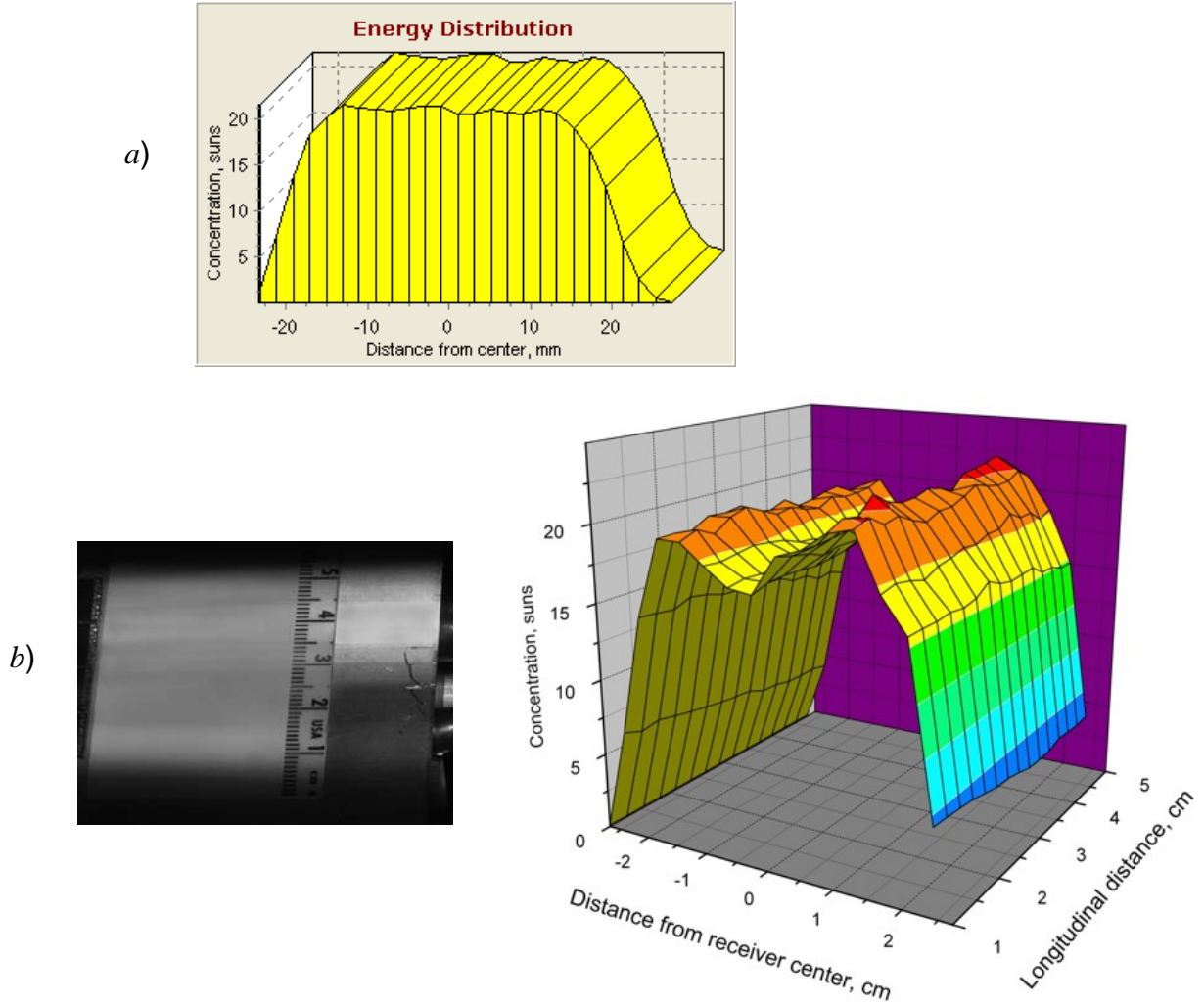


**Figure 51. Comparison of calculated (a) and actual (b) flux maps**

Photo Credit: SVV Technology Innovations

The analysis of irradiance distribution revealed a notable improvement in concentration and uniformity obtained with the focus improver (see Figure 52). The focus improver also ensured that energy spillage due to the optics and tracking errors is minimized. A comparison of the total energy collected in a 4 cm (1.6 in) strip corresponding to the width of PV cells shows that the focus improver brings 5 to 10% of the concentrated flux back to the receiver. Without it, the corresponding fraction of incident solar radiation would have missed the cells.

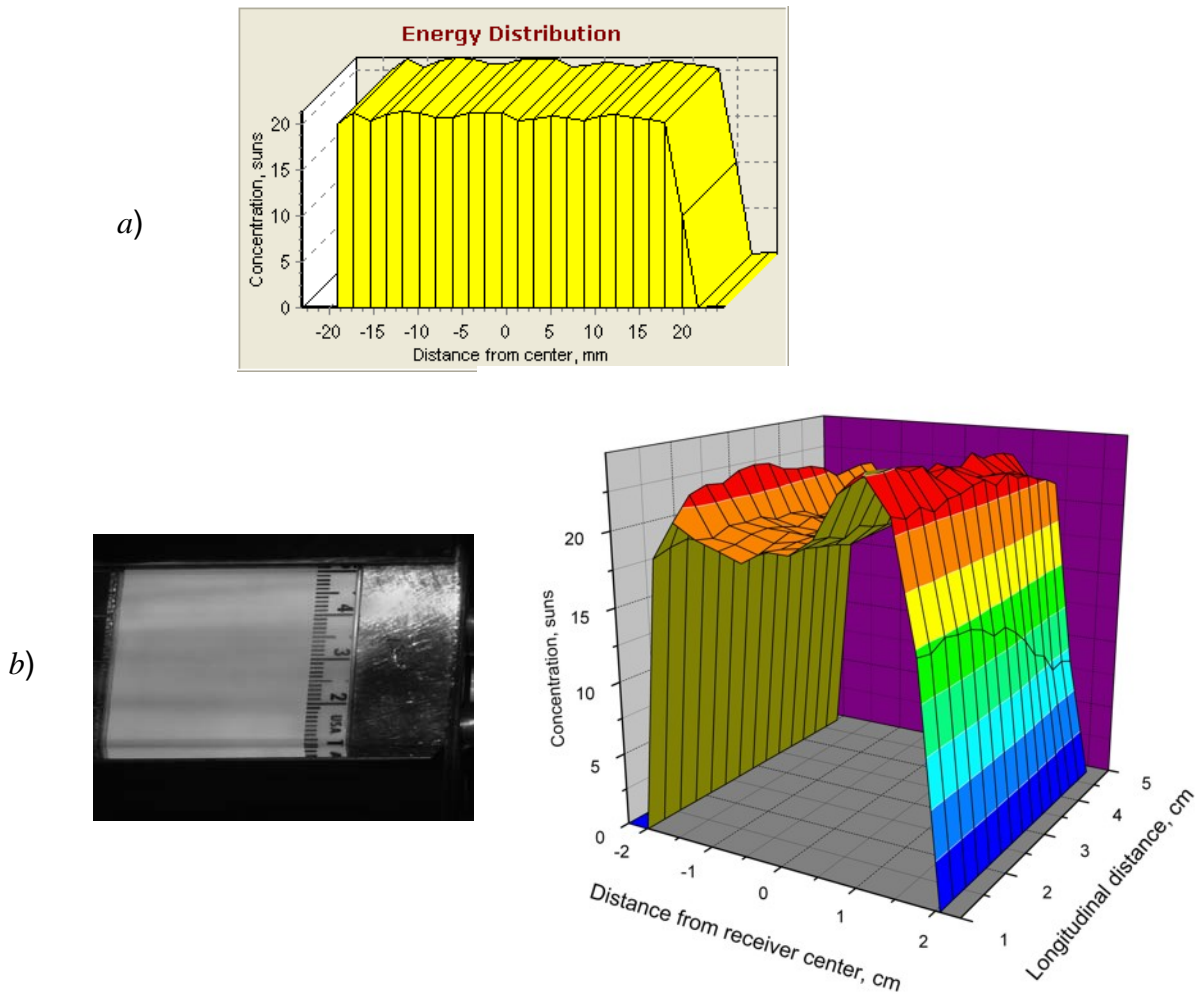


**Figure 52. Calculated (a) and actual (b) flux maps with focus improver**

Photo Credit: SVV Technology Innovations

### **Power output**

The optical concentration and power output were also evaluated from the electrical measurements using the test PV receiver placed in the concentrator's focus. Figure 53 shows the electro-optical test receiver exposed to an average 20-suns concentration.

Electrical measurements were conducted with the test PV receiver to obtain the short circuit current values at different illumination levels, as well as I-V dependencies. The I-V curves were used to estimate the maximum electric power output. The temperature of the PV cells was kept nearly constant in the range of 25°C to 30°C (77°F to 86°F) due to active water-cooling.

Table 4 shows the expected and actual electrical parameters of the four-cell receiver. The measurements of  $I_{sc}$  and peak power obtained at about 900 W/m<sup>2</sup> insolation levels are extrapolated for the standard one-kW/m<sup>2</sup> flux.

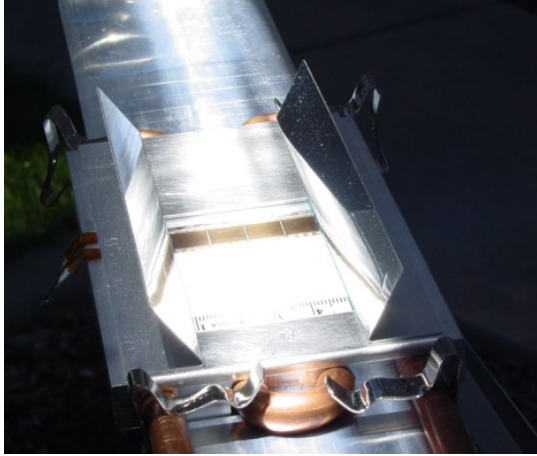


**Figure 53. Test receiver based on high-efficiency PV cells**

Photo Credit: SVV Technology Innovations

**Table 4. Comparison of measured and expected performance of PV**

Parameter	Rated/Expected	Measured
1 sun		
Peak Efficiency	25%	N/A
Short Circuit Current ( $I_{sc}$ ), A	N/A	12.3
Open Circuit Voltage ( $V_{oc}$ ), V	N/A	9.9
20 suns		
Peak Efficiency	28%	N/A
Short Circuit Current ( $I_{sc}$ ), A	0.24	0.21
Open Circuit Voltage ( $V_{oc}$ ), V	10.4	10.2
Peak Power Output, W	2.2	1.9

Source: Data collected by Sergey Vasylyev

The observed difference between expected and measured values in the short circuit current corresponds to the optical losses in the concentrator, and conforms well to previous estimates of the concentrators' efficiency. The table shows the expected magnitude of the open circuit voltage of 10.4 V at 20 suns, which differs from previous estimates of 11 to 12 V. This is because the old estimates were based on the factory-provided data for 500 suns concentrations, which can be associated with higher voltage magnitudes. Some newer data provided by the cell's manufacturer suggests that  $V_{oc}$  for a single cell should be about 2.6 V at 20 suns, which makes a closer estimated value for a four-cell receiver of 10.4 V. This value also agrees more closely with our measurements performed for the non-concentrated (ambient) sunlight as well as 20 suns concentrated flux.

The analysis of the data confirms the high optical efficiency of the system, and shows the specific power of 1.9 W per centimeter length of the linear PV receiver based on triple-junction solar cells. As the cells of the test receiver cover only about 0.35% of the total focal area of the prototype CPV, the research team estimates that this system would generate over 530 watts of peak power, provided the PV receiver is extended to the full size of the concentrator's focal area.

The triple-junction cells used for this prototype use side electrical contacts which occupy a substantial fraction of the cell area (more than 25%). Therefore, if the receiver can be made with a higher packing factor for the cells, the total power output can be further increased.

### ***Wind resistance***

The SAC concept replaces the large area of a conventional mirror with an array of reflectors that have substantial gaps between them. This leads to a significant reduction of the wind drag per concentrator unit area, as well as the utilization of a more lightweight structure. A photograph in Figure 54 shows another view of the tracker mounted final prototype SAC, demonstrating the open frame structure of the design, which can effectively deflect relatively high winds.



**Figure 54. The concentrator designed to deflect wind loads**

Photo Credit: SVV Technology Innovations

One of the earlier concerns regarding the concept was that the larger concentrator, utilizing relatively long and narrow slats, would exhibit some flutter of its mirror that could affect its performance. Therefore, the monitoring schedule also included days with relatively high winds, which were abundant at the Elk Grove, California, site.

The observations revealed no fluttering of slats, which could result in performance degradation at winds up to 42 to 48 km/h (26-30 mph), the strongest winds that occurred during the monitoring period. The overall SAC structure was also unaffected. The tracker itself is designed to withstand wind loading of 129 kg/m<sup>2</sup> (32 lbs/ft<sup>2</sup>) over 145 km/h (90 mph) and hold a flat-plate PV panel of up to 21 m<sup>2</sup> (225 ft<sup>2</sup>). Since the slat-array CPV has a relatively low wind drag, we estimate that an equivalent area of the SAC CPV modules totaling over 3.7 kW of power capacity can be installed on this tracker, representing a 20-fold reduction of PV cell area compared to flat plate modules.

### ***Effects of soiling***

The prototype SAC was exposed to the outdoor conditions for a period of about three weeks, with periodical maintenance and mirror cleaning while conducting tests. As with the small prototype, the reflective surfaces of concentrator slats experienced much less soiling than the surrounding surfaces. This was partially due to the fact that the slats were inclined with respect to the horizon most of the time during the day, and in the stowed position of the concentrator at night. Also, the reflective material of the slats is based on a pure aluminum substrate which helps to maintain antistatic properties and repel dust.

Even after almost a weeklong exposure without mirror cleaning, the concentrator performance remained high and the degradation of power output with the test receiver was in the range of measurement errors. However, after a rainy day, the effects of soiling were notable and the concentrator had to be cleaned. Horizontally positioned slats were most affected. A cleaning of the concentrator restored the original optical efficiency completely, allowing the team to obtain consistent results before and after cleaning. While the slat-array mirror may need less frequent cleaning than, a parabolic trough, mirror washing is still required on a regular basis, as with all reflective concentrator.



## 3.0 Project Outcomes

The goal of this project was to explore new technical solutions for more efficient collection of solar energy for power generation and reducing dependence on conventional (non-renewable) sources of energy.

By building and testing the world's first slat-array concentrator, this project demonstrated a new way to collect the solar energy using novel optical systems, which are more advanced and technologically friendly than traditional methods.

It was demonstrated that the new SAC, composed of an array of simple concave slats, offers high optical efficiency and performs similarly to parabolic mirrors, today's most effective solar concentrators. Also, the new concept allows us to realize significant savings in weight and fabrication costs of the concentrator and its support structure, when compared to the traditional reflective solar collectors.

### Technical Objectives

1. Demonstrated the feasibility of the SAC and fabricating the first-of-its-kind CPV module based on this concept. The demonstration of workability of the SAC concept was a major goal of this project. Both modeling and experimental data gathered in this project provide valuable information about the optical performance of SAC and its other technical characteristics.
2. Demonstrated that solar energy can be concentrated by at least 20 to 40 times on PV cells interconnected and arranged in a continuous strip, without overheating the central portions of the cells, while maintaining high solar to electric conversion efficiency.
3. Built a larger, 2.79 m<sup>2</sup> (30 ft<sup>2</sup>) SAC module designed for 500 Watt-peak (Wp) output and moderate sunlight concentration. This module can serve as a prototype for future commercial CPV systems.

While further research is needed in this area, by designing and developing a new 500 W CPV module based on the SAC collector coupled to a PV array, the project team demonstrated a prototype device which can be a building block for tomorrow's electricity generation systems.

There is evidence from the results of this study that the new solar concentrator can be used extensively in a wide range of applications where sunlight collection is required, and the cost and portability of the underlying collector technology is an issue.

The new solar concentrator offers a unique blend of features which, in this useful combination, cannot be found among the existing high-flux concentrators (see Table 5). This could further increase the cost competitiveness of solar technologies.

**Table 5. PV Concentrator Technology Comparison**

<b>Concentrator Characteristics</b>	<b>Linear Fresnel Lens</b>	<b>Parabolic Trough</b>	<b>SAC</b>
<b>Concentration, suns</b>	< 20	20+	20+
<b>Back Focus/ Unlimited Receiver Size</b>	Yes	No	Yes
<b>Unlimited Module Size</b>	No	Yes	Yes
<b>Flux Uniformity</b>	No	No	Yes
<b>Mass Producing by Existing Industry</b>	Yes	No	Yes

Source: Data collected by Sergey Vasylyev

Through numerous experiments and iterations, the authors developed an original fabrication method for high-concentration 500 W CPV modules, which employs only straight or radius-bent shapes, simple manufacturing techniques, with widely available industrial materials. In order to minimize weight, the prototypes were produced with aluminum components. Similar structural steel shapes could be used, which could further reduce material, fabrication, and production costs.

The research team also identified various methods for the mass production of the SAC module components. The authors concluded that a low-cost, continuous manufacturing process, such as industrial roll-forming, can be used for producing SAC mirrors.

The results of this project were presented at the annual meetings of the American Solar Energy Society (ASES) in Austin, Texas (June 21 through June 26, 2003) and Portland, Oregon (July 9 through July 14, 2004). The corresponding papers were published as a part of conference proceedings (Vasylyev 2003; Vasylyev 2004).

## 4.0 Conclusions and Recommendations

### 4.1 Conclusions

Under this project, SVV Technology Innovations, Inc. developed a prototype CPV device based on the Slat-Array Concentrator, and demonstrated its performance.

An optical efficiency of about 85% was obtained for the prototype concentrator, and solar to electric efficiencies of up to 22% were measured for a CPV module based on this SAC. A weight to aperture ratio of 10 kg/m<sup>2</sup> (2.5 lbs/ft<sup>2</sup>) was obtained for the final prototype SAC module.

The development, monitoring, and evaluation of the final SAC prototype proved that a commercial-size CPV system, with over 500 Wp capacity, can be built using the concept of the SAC. The results demonstrated that the system can be scaled up without sacrificing optical advantages, and that the use of Slat-Array Concentrators can reduce PV cell area by 20 to 40 times, while maintaining relatively high solar to electric conversion efficiency. The CPV module can serve as a prototype for future commercial systems generating distributed electrical power.

The targeted technical performance achieved for the SAC in this project indicate that the studied concept offers a technical advantage in efficient solar collection. The initial estimates of the production costs of the SAC suggest that one can fabricate cost-effective CPV modules for generating “green” electricity that contribute to Public Interest Energy Research (PIER) program objectives.

While the goals for this project were achieved, there is a need of further Research, Development, and Demonstration (RD&D) and improvements in the manufacturing process for key SAC components and the product as a whole.

### 4.2 Commercialization Potential

The commercialization potential of the SAC is supported by the growing worldwide demand for solar collector technologies, converting freely available solar energy to electricity directly, or offsetting electric energy consumption by providing an alternative source of concentrated heat.

The SAC seeks to be a superior alternative to the conventional high-flux concentrators, such as parabolic troughs and Fresnel lenses, for a wide range of solar applications. Therefore, to a significant degree, the market prospects of the SAC are commensurate with the demonstrated advantages of this new concept over existing products in this range of concentrations.

#### 4.2.1 Comparison to Parabolic Troughs

The SAC is essentially a linear-focus reflector, just like the parabolic trough. Therefore, comparing it to the trough, being the best-known and least expensive high-flux solar concentrator today, is most appropriate for assessing the feasibility of the new concentrator design.

##### ***Mirror***

In a conventional parabolic trough mirror, reflective material is attached to at least one layer of 1.5-mm (0.06 in) or thicker aluminum or steel substrate, providing additional rigidity. However, the thickness of this sandwiched mirror is usually not enough to hold the perfect parabolic shape

without additional support. Therefore, a system of transversal ribs attached to a support structure, repeating the shape of the parabola, is typically required.

In the SAC, each slat has a transversal profile several times shorter than the trough's. As a result, the necessary curved shape can be maintained with a significantly thinner mirror. In the prototype SAC, the substrate layer was even completely eliminated. The proper structural rigidity of 0.5-mm (0.02 in) reflective aluminum was sufficient to hold the circular slat profiles.

The suitable stiffness and rigidity of slats is obtained by reinforcing them with simple longitudinal ribs fabricated from strips of 0.3mm (0.012 in) thick aluminum coil. The coil is very lightweight and inexpensive so it does not add much to the cost and weight of the reflector. The ribs are attached to the slat back in the shadow zone, so that no shadowing of the concentrated flux is introduced.

Due to skewed positioning of slats, the SAC utilizes about 30 to 40% more reflective laminate material than the trough, depending on the trough's aperture ratio. However, as sufficient structural rigidity is achieved in SAC with less metal, the increase in laminate area consumption is offset and actually reduces system weight compared to troughs.

The most lightweight trough reflectors typically weigh from 6 to 12 kg/m<sup>2</sup> (1.4-2.8 lbs/ft<sup>2</sup>) of active aperture. As was noted above, the reflector of the prototype SAC weighs only 3 kg/m<sup>2</sup> (0.7 lbs/ft<sup>2</sup>). The reflector with reinforcement, providing superior rigidity and shape stability, weighs 4.2 kg/m<sup>2</sup> (1 lbs/ft<sup>2</sup>), still considerably less than the weight of non-reinforced trough reflector.

### ***Optics and performance***

The parabolic troughs are based on a traditional optical scheme employing a large continuous surface in a parabolic profile. Such a profile is ideal for imaging and collecting parallel rays coming from a distant point source. However, the sun is not a point source and its finite angular size (about 0.5°) causes distortion of concentrated flux, due to off-axis optical aberrations, and puts a fundamental limit on concentration. Additionally, the parabolic profile is difficult to maintain for a large mirror, where even the smallest imperfections in shape can result in further decrease of concentration.

The cylindrical troughs that have a circle-shaped transversal profile can be somewhat easier to manufacture and maintain. However, they are less practical, since the off-axis optical deviations of such systems are more significant. These result in much lower concentrations compared to parabolic troughs.

The SAC mirror exploits a different optical concept, aimed at the most efficient collection of sunlight for a given size receiver. Rather than forming crisp images, it uses an array of relatively narrow slats and non-imaging optical principles to reduce the effects of off-axis aberrations and further increase the concentration. The SAC is still utilizing only a single reflection, introducing no secondary optics.

Furthermore, the current version of the SAC under study completely departs from the idea of using a complex parabolic shape. Instead, it employs much simpler, circular profiles for the slats, where most of the slats have identical curvatures.

As demonstrated in this project, the optical performance of a prototype concentrator based on the SAC concept compares to that of the best parabolic troughs. The optical performance of the SAC is determined chiefly by the selection of material reflectivity and slat manufacturing technique. Specifically, the authors estimate that the optical efficiency of SAC can exceed 90% if a 95%-reflective laminate is used and slats are manufactured in a high volume batch process.

Compared to the continuous-surface reflector of a parabolic trough, notable edge effects affecting the concentrator performance have not been observed for the SAC prototypes which have multiple reflectors. The concentrator optical efficiency obtained from independent measurements is estimated to be about 85%, which agrees with model estimates. Therefore, the research team assumes that these edge effects, if any, do not exceed 1 to 2%, as originally predicted.

The project has demonstrated the validity of theoretical calculations and computer modeling by designing a PV version of the SAC with moderate concentrations. Further computer modeling with the same approach shows that linear-focus concentrators, with record concentration ratios of 100 to 200 suns, can be built. This is well beyond the limits of parabolic troughs.

The improved uniformity of the concentrated solar flux, as demonstrated in this project, is a unique feature, which is not found among trough-like concentrators that do not use secondary optics. While uniformity was achieved due to some sacrificing of the concentration ratio, the obtained concentration of 38 suns for the prototype SAC is still one of the highest concentrations reported to date for similar linear-focus SAC systems (see, for example, Sala et al. 2000; Smeltink et al. 1999; Weatherby and Bentley 1998).

As other theoretical and experimental studies show, when a parabolic trough is used with concentrator PV cells, 30 to 40 suns geometrical concentration is typically accompanied by a hot spot in the receiver center, where the peak concentration can triple and the irradiance can easily exceed 100 suns. This can cause immediate damage to the PV cells that are designed for less intense fluxes, as well as significantly reduce system performance and reliability.

SAC solves this key issue of hot spots by flattening the energy profile across the focal line, while maintaining high concentration. As ray tracing demonstrates, a uniform energy distribution can be obtained without the use of secondary optics. Experiments with prototype SACs confirm notable improvement in flux uniformity, which helps remove hot spots on the cells and thus preserves efficiency. Uniformity can also provide the opportunity for using less expensive cells and possibly use of conventional one-sun PV cells used in flat plate modules.

### ***Support frame***

The support structure is very important to consider in solar concentrator cost estimation. The structure is often responsible for 40 to 65% of the total cost in all kinds of concentrating systems. According to numerous cost analysis available on parabolic troughs, the mirror support can cost two to three times more than the mirror itself.

The support frame of parabolic troughs needs to be manufactured to repeat the parabolic shape with very close tolerances that are hard to achieve in a large scale design. This means significant weight and cost. As the parabolic trough is practically a perfect "sail," the structure needs to be

particularly massive to withstand high wind. In commercial trough designs, the weight to aperture ratio is typically 14 to 40 kg/m<sup>2</sup> (3.5 to 10 lbs/ft<sup>2</sup>).

In the SAC, a simple space frame structure can be integrated into the concentrator design, which saves on weight and costs. As the reinforced slats are rigid enough, no additional support for keeping the needed shape for the mirror is required. Additionally, the slats are inclined at an acute angle to the aperture plane, and so deflect wind and rain more efficiently than a large-area concave surface, allowing free passage of air and water between the slats.

In the SAC prototype, the support frame for both concentrator and PV receiver weighed about 30 kg (80 lbs), which translates into 10 kg/m<sup>2</sup> (2.5 lbs/ft<sup>2</sup>). This can reduce the CPV system cost by 25 to 30% in comparison to other concentrators.

### ***Tracking***

The prototype concentrator developed in this project was intended to be operated with a dual axis tracker. These trackers can be optimized for concentrating PVs, capturing a maximum amount of energy with a minimum of cell and concentrator area.

On the other hand, the SAC optics performs similarly to a parabolic trough when tracked around one axis. Therefore, it can be successfully used in most thermal applications where parabolic troughs are traditionally employed. When designing the SAC for single-axis tracking, a different method for slat mounting can be used, in order to minimize partial flux shadowing by sidewalls utilized in the current prototype. The ASEND software easily adapts the system parameters for the various needs of the concentrator.

The tracking tolerances for the SAC and a trough are similar for the equivalent focal distance. In particular, experiments have shown that the precision of 0.1° to 0.3°, offered by today's commercially available two-axis trackers, is sufficient for mid-concentration PV systems. Computer modeling has shown that the optical scheme of the SAC allows for a shorter focus than a parabolic surface with the same aperture. Therefore, even lower tracking precision can be employed.

### ***Manufacturing***

As experimentally confirmed in the project, reflective slats can be easily manufactured with a variety of widely available means and materials.

The fabrication of slats, including their lamination with a reflective film, can be set up as a continuous and fully automated process, something that can be very difficult for commercial-size troughs and other conventional reflectors. Currently, there are only a few trough manufacturers in the world and, until recently, there was only a single manufacturer in the United States. In a large part, this is due to the inherent complexity of parabolic trough technology.

The replacement of the parabolic cross-sectional profiles of slats with “technologically friendly” circular ones provides an opportunity to expand the manufacturing opportunities even further. The cylindrically shaped slats can now be manufactured in a batch process of slip rolling, roll forming, or other simple techniques. This brings the cost of slat manufacturing close to the cost of material itself.

As the team demonstrated in this project, SAC manufacturing can be affordable even for small shops and labs, since conventional bench top tools can be used to complete the entire cycle of fabrication. Other inexpensive fabrication techniques, such injection molding, stamping, etc., can also be successfully used, especially for smaller modules and larger quantities.

In a trough, the parabolic shape of the mirror is maintained by a support frame, which requires very close tolerances for the entire support structure. The assembly of a trough, especially on the site, requires relatively qualified labor. By comparison, the SAC has a low-tech Venetian-blind structure, offering simple assembly and disassembly, as well as very compact packaging opportunities.

The design of the SAC allows for further savings in the reflector since the slats can be fabricated from a larger variety of materials including plastics, which are quite problematic for large-area troughs. Additionally, some lower-grade plastics can be employed since the reflectivity typically increases in dielectrics at skew angles of incidence.

### ***Soiling***

Cleaning the SAC reflector can be somewhat more difficult than cleaning a trough, which has a less elaborate surface. However, due to the nature of SAC design, the slats remain inclined to the horizon at all times when in operation, which makes them less exposed to soiling compared to the troughs which face upward. For example, high soiling rates of 0.5% to 3% per day have been reported for troughs (see Sala et al. 2000; U.S. DOE 1997). For comparison, a two-week outdoor exposure of an SAC in a windy area with heavy residential construction, resulted in very light reflector soiling, while the surrounding flat surfaces became substantially covered with dust during the same period. Further long-term study in soiling is needed for the SAC.

### ***Operation and Maintenance***

SAC offer a true lens-like functionality, allowing for better operational conveniences compared to a trough due to easier access to the focus. The focus is disposed on the rear, which does not block the incident flux.

Even a tiny deformation of the shape of parabolic trough may result in significant distortions of the focal spot and make the mirror unusable. When the continuous-surface mirror is physically damaged, it has to be replaced entirely, which involves all the costs associated with a new mirror and labor for its installation.

By comparison, the slats in the SAC are independent of each other. Therefore, damage to a single slat results only in the distortion of a small portion of the concentrated flux associated with that slat. Even the removal of a slat will only drop the efficiency by a small percentage and will not affect the operation of the rest of slats. The SAC can also be designed to allow for individual slat replacement without disassembly, which can further reduce the maintenance costs.

The preliminary results of computer modeling, and actual experiments with slat alignment, show that the relatively high-magnitude random imperfections in shape or position of individual slats (e.g., 100 mrad, or  $5.73^\circ$  in angular position and 15 to 20% in the radius of reflective surface

curvature) result primarily in uniformity degradation and some minor spillage of energy, while the net concentration ratio degrades insignificantly for a given intercept factor. For comparison, a deviation in the curvature of a parabola of 15% can destroy its focus.

Because the required tolerances to macro imperfections of the SAC reflector are several times less compared to the traditional troughs, a field of collectors based on slat-array optics can operate more reliably and effectively.

#### **4.2.2 Comparison to Fresnel Lenses**

Despite the fact that Fresnel lenses are considered less efficient and less practical for solar thermal applications compared to reflectors, they have been increasingly used for concentrator PVs due to their relative low cost and more convenient operation compared to retro-reflecting mirrors. Because the SAC operates like a lens, such a comparison is appropriate.

Refractive lenses, like a Fresnel lens, have two fundamental limitations in some of the most important characteristics for solar optics: the concentration ratio and the size. The practical limit of sunlight concentration achievable using linear-focus Fresnel lenses is about 20 suns. The main reasons are the low refraction index of available transparent plastics, chromatic aberrations, and inherent optical losses. Most commonly, the concentration varies from roughly 10 to 16 suns for these systems. Thus, the SAC has an advantage in a CPV system, since it has the potential for several times greater PV cell area reduction compared to Fresnel lenses.

Another known limitation of Fresnel lenses, owing to the increase of refraction losses at their peripheral zones, leads to a maximum practical lens size of about 80 to 90 cm (less than 3 feet). The SAC does not have this limitation and can even be manufactured to aperture sizes several times greater than parabolic troughs.

Even for smaller sizes, the optical efficiency of a typical Fresnel lens concentrator is 80%, which is several percent less than that of the SAC. Therefore, the SAC with efficiency of 85% or higher will generate several percent more electricity for the same active aperture, same amount of PV materials, compared to a lens-based device.

For lower concentrations, 20 suns and below, the SAC also has certain advantages. The lower requirements for optics in this concentration domain allow for even further simplification of the SAC optics, further reducing potential manufacturing cost. For example, all cylindrically shaped slats in the SAC can be identical, so that a single process can be used for fabrication.

Fresnel lenses form non-uniform concentrated fluxes. As a matter of refractive optics, the flux distribution also varies from one spectral domain to another. Therefore, providing uniform receiver illumination is not possible for lenses without using secondary concentrators thus incurring additional energy losses and costs. For comparison, the SAC adds no spectral dispersion and can provide uniform fluxes using no secondary concentrations.

The wholesale prices for ordinary optical-grade Fresnel lenses are ranging from about \$50 to \$100/m<sup>2</sup>, more than the material cost of an SAC reflector manufactured from high-grade aluminum (\$40/m<sup>2</sup>).

The selection of materials for lenses is essentially limited to acrylics. No such limitation exists for the SAC because the slats can be made of metal, plastic, or glass. For less demanding applications, a less expensive grade of reflective aluminum can be utilized at the cost of \$11/m<sup>2</sup>. In some cases, even much cheaper materials, such as HiFi-MET, costing \$1.9 to \$2.6 per m<sup>2</sup>, can be utilized at the expense of some reduction in efficiency and weatherability.

### **4.3 Recommendations**

The results of this PIER-funded project demonstrate that the SAC concept is an ideal choice for concentrating PV in a wide range of concentrations. The system has been shown to overcome deficiencies commonly associated with solar concentrators such as size, flux uniformity, durability, and maintenance, while also showing great potential for reducing the cost of collecting and converting solar energy into electricity.

With only a few market-entry CPV products being commercially available today, further RD&D effort is needed for the creation of a robust commercial product. It will incorporate the best possible SAC fabrication technology, a suitable PV receiver, and a matching sun tracking system in order to offer a viable commercial product.

The concept of the SAC is relatively new compared to the well-known solar collector concepts and products employing mirrors and lenses. Because the SAC has demonstrated a number of optical advancements and operational advantages, a further refinement of this concept is needed to fully exploit its benefits and determine the applicability limits.

Follow-on projects that provide an ideal match between the SAC design and commercially available PV cells should be developed. A further study of the leading brands of monocrystalline PV cells is needed to identify the best performing products under moderate sunlight concentrations.

The scope of this project should be expanded to retrofit the SAC design for other concentrating solar power applications, such as the parabolic trough technology, which today accounts for 50% of all electricity generated from solar worldwide. This will allow the authors to spread the cost saving advantages of SAC collectors to a broader variety of renewable energy technologies.

### **4.4 Benefits to California**

The result of this work contributes to the PIER Program objectives of developing a new generation of low-cost renewable technologies, through the development and demonstration of a new Slat Array Concentrator, and CPV prototype module. It also contributes to the development of the solar energy industry, which is supported by the overwhelming majority of Californians.

The solar-electric implementation of the SAC, once commercially available, could expand the PV market by providing a lower-cost alternative to conventional and emerging CPV technologies. The system, weighing about the same as a flat-plate PV module, provides a 20 to 40 times reduction in PV cell consumption with a corresponding reduction in silicon usage for the PV cells. Concentrator cells manufactured in California provide higher solar to electric efficiencies, with

corresponding higher levels of concentration. This helps to harness the highest potential of PV technology and provides a potential sustainable domestic source of clean energy.

In addition, future products based on the SAC, such as solar thermal collectors, water heaters, desalinators, chillers, etc., will become more effective and more marketable as the SAC develops. Finally, California's electric ratepayers will benefit from the increased amount of electricity generated from renewable sources, reducing the peak demand for grid-supplied electricity, and the likelihood of electricity shortages.

## Nomenclature

$B$  – solar limb brightness;

$\theta_p$  – positional angle of the sun;

$\theta_c$  – angular distance from the center of the sun;

$C_G$  – geometrical concentration;

$A_C$  – concentrator entrance aperture;

$A_R$  – receiver entrance aperture;

$C_{RAW}$  – raw concentration;

$FF$  – fill factor;

$\eta_{opt}$  – optical efficiency of concentrator;

$F_{D\ concentrated}$  – direct solar irradiance of a receiver under concentration;

$F_D$  – direct solar irradiance of a receiver (no concentration);

$I_{sc}$  – short circuit current;

$V_{oc}$  – open circuit voltage;

$I_{DC}$  – DC current;

$V_{DC}$  – DC voltage;

$F_G$  – global solar irradiance;

$\eta_{cell}$  – solar to electric conversion efficiency of a PV cell;

$\eta_{CPV}$  – solar to electric conversion efficiency of a CPV device;

$k_T$  – temperature coefficient for  $I_{sc}$ ;

$I_{sc\ concentrated}$  – short circuit current of a PV cell under concentration;

$k_{\Delta\theta}$  – coefficient reflecting the optical effects of off-normal incidence angles  $\theta$ ;

$P_I$  – light power incident to the cell aperture;

$I_{mp}$ ,  $V_{mp}$  – current and voltage corresponding to a maximum power output of a cell,

respectively;

$A_C$  – concentrator aperture;

$P_{IC}$  – direct incident energy collected by concentrator;  
 $N_e$  – electron-counts per pixel;  
 $N_c$  – CCD-recorded signal (counts);  
 $G$  – CCD camera gain;  
 $k_C$  – gray level to surface irradiance conversion factor;  
 $C_A$  – concentration level corresponding to a pixel;  
 $F_{G-1SUN}$  – one sun surface illumination;  
 $N_{C-1SUN}$  – CCD signal level corresponding to one sun illumination;

## References

Sala, G., Antyn, I., Arboiro, J.C., Luque, A., Cambor, E., Mera, E., Gasson, M.P., Cendagorta, M., Valera, P., Friend, M.P., Monedero, J., Gonzalez, S., Doby, F. 2000. The 480kW<sub>peak</sub> EUCLIDESTM—THERMIE Power Plant: Installation, Set-Up and First Results. Proceeding of the 16th European Photovoltaic Solar Energy Conference and Exhibition, WIP—Stephens & Associates, Glasgow, Scotland.

Smeltink, J., Blakers, A.W. and Hiron, S. 1999. The ANU 20kW PV/Trough concentrator. In Proceedings, Solar 99, Melbourne, Victoria.

U.S. Department of Energy (DOE), Office of Utility Technologies and the Electric Power Research Institute, Inc. 1997. Solar Parabolic Trough, in Technology Characterization, TR-109496.

Vasylyev, Sergey 2003. Development of a Slat-Array Photovoltaic Concentrator. Proceedings of Solar 2003 National Solar Energy Conf., Austin, Texas.

Vasylyev, Sergey 2004. Performance Measurements of a Slat-Array Photovoltaic Concentrator. Proceedings of Solar 2004 National Solar Energy Conf., Portland, Oregon.

Weatherby, C K and R W Bentley. 1998. Further Development and Field Test Results of Two Low-Material-Cost Parabolic Trough PV Concentrators. Proceedings, 2nd World Conference on PV Solar Energy Conversion, Vienna, 2, 2189-2192.



## Glossary

AC	Alternating Current. A type of electrical current that changes direction at regular intervals. In the US, the standard frequency is 60 cycles per second.
Amorphous Silicon	A thin-film, silicon photovoltaic cell material having no crystalline structure, manufactured by depositing layers of PV material on a glass or metal substrate.
BOS	Balance of System, the components that comprise a complete PV system other than the PV module(s). The BOS includes items like the inverter, module support structure, wiring, conduit, hardware, protection equipment and switches.
Cell	Building block of photovoltaic systems, a small piece of material that creates voltage, current, and thus electrical power, when in sunlight.
CNC	Computerized numerical control.
CPUC	California Public Utilities Commission, which regulates privately owned electric, telecommunications, natural gas, water, and transportation companies, in addition to household goods movers and rail safety.
CPC	Compound parabolic concentrator.
CPV	Concentrating photovoltaic.
Current	A flow of electric charge.
DC	Direct Current. A type of electricity by which electricity flows in one direction and is usually a relatively low voltage and high current. Autos have a DC electrical system with a DC battery. Photovoltaic modules produce DC electricity.
Direct sunlight	Portion of sunlight that is capable of being concentrated. On a clear day, 80 to 95% of sunlight is direct.
Energy Commission	California Energy Commission, or CEC ( <a href="http://www.energy.ca.gov/">http://www.energy.ca.gov/</a> ).
ERP	Emerging Renewables Program, of the California Energy Commission program whose goal is to develop a self-sustaining market for "emerging" renewable energy technologies in distributed generation applications. The program was created to stimulate market demand for renewable energy systems that meet certain eligibility requirements by offering rebates to reduce (buy down) the initial cost of the system to the customer.
FF	Fill factor, being defined as the ratio of the peak power to the product $I_{sc}$ and $V_{oc}$
Focal plane	The plane that is perpendicular to the axis of the lens and passes through its focus.
Fresnel lens	A thin optical lens consisting of concentric rings of segmental lenses and having a short focal length, used primarily in spotlights, overhead projectors, and the headlights of motor vehicles.
Flux	Solar radiation hitting a surface.
Grid (Electrical grid)	An integrated utility system of electricity generation

	and distribution consisting of the wires, transformers, substations, power plants and control systems. The grid may also refer just to the transmission and distribution system, not including generation, particularly in regions where generation is owned by separate entities.
Heat sink	A protective device that absorbs and dissipates the excess heat generated by a system.
IF	intercept factor.
Insolation	The rate of delivery of solar radiation per unit of horizontal surface.
IOU	Investor Owned Utility, owned by shareholders.
kW	Kilowatt
A standard unit of electrical power equal to 1,000 watts, energy flow at a rate of 1000 joules per second.	
kWh	Kilowatt-hour. 1,000 thousand Watts acting over a period of 1 hour. The kWh is a unit of energy. 1 kWh=3,600 kilo Joules.
MW	Megawatt. 1,000 kilowatts, or 1 million Watts, a standard unit of electric power plant generating capacity.
NEC	National Electrical Code, which contains guidelines for all types of electrical installations. The NEC contains Article 90, "Solar Photovoltaic Systems" which should be followed when installing a PV system.
NREL	National Renewable Energy Laboratory, the primary federal laboratory for renewables, located in Golden, Colorado.
Non-imaging reflective lenses	Rear-focus concentrator design based on an array of mirrored elements.
Parabolic mirror	A concave mirror that has the form of a paraboloid of revolution.
Peak Load	The highest electrical demand during a particular period of time. Daily electric peaks on weekdays usually occur in late afternoon and early evening. Annual peaks typically occur on hot summer days.
PG&E	Pacific Gas and Electric Company. An investor owned gas and electric utility covering much of northern California.
Power	A product of voltage and current.
PV	Photovoltaic. The term used for the conversion of sunlight to electrical energy usually through the use of a PV cell, a semiconductor device.
PV Array	An interconnected system of PV modules that function as a single electricity-producing unit. The modules are assembled as a discrete structure, with common support or mounting. In smaller systems, an array can consist of a single module.
PV Module	The smallest environmentally protected assembly of solar cells.
PV System	A complete set of components for converting sunlight into electricity by the photovoltaic process, including the array and balance of system (BOS) components.

Public Goods or Benefits Funds

Public Benefit Funds are state-level programs usually developed as part of a utility restructuring process to continue support for renewable energy resources, energy efficiency initiatives, and low-income support programs. These funds are sometimes called a *system benefits charge*. Such a program is most commonly funded through a consumption charge to all electric customers, e.g., 0.2 cents/kWh. Examples of how the funds are used for PV include: rebates on renewable energy systems; funding for renewable energy R&D; and development of renewable energy education programs.

Ray tracing

In computer graphics, an advanced technique for adding realism to an image by including variations in shade, color intensity, and shadows that would be produced by having one or more light sources.

RPS

Renewable Portfolio Standard, a requirement that a certain percentage of a utility's overall or new generating capacity or energy sales must be derived from renewable resources. For example, one percent of electric sales must be from renewable energy. The term "set asides" is frequently used to refer to an RPS in which a utility is required to include a specific amount of a certain renewable technology (such as solar).

SAC  
SDG&E

Slat-Array Concentrator.

San Diego Gas and Electric Company, an investor owned gas and electric utility covering much of the southern part of California.

SCE

Southern California Edison, an investor owned electric utility covering much of the area around Los Angeles and the south central portion of California.

SFPUC

San Francisco Public Utility Commission, a department of the City and County of San Francisco that provides water, wastewater, and municipal power services to San Francisco.

Silicon

A nonmetallic element occurring extensively in the earth's crust in silica and silicates, used extensively in the production of photovoltaic cells.

Slats

A narrow strip of metal or wood, as in a Venetian blind.

SMUD

Sacramento Municipal Utility District, the municipal electric utility in Sacramento, California that provides electric power to Sacramento County (and a small part of Placer County) at competitive rates that are consistently lower than investor-owned utilities in the state. SMUD is the sixth largest publicly owned utility in the country in terms of customers served. SMUD's mission is to provide value for their community while working to improve the quality of life in Sacramento.

Specular reflectivity

Of, resembling, or produced by a mirror or speculum.

STC

Standard Test Conditions, under which a module is typically tested in a laboratory. The conditions

Suns	include a temperature of 25°C, and an irradiance of 1,000 watts per square meter.
Sun tracking	Concentration of multiple values of one sun. Following of the sun across its daily path for solar energy collection purposes; sun-tracking with one axis of rotation, or sun-tracking with two axes of rotation.
Solar thermal	At present, applications for heating swimming pools, heating water for domestic use, and space heating of buildings typically using flat-plate or evacuated tube collectors with a fixed orientation. Higher concentrated solar thermal energy collection is used for refrigeration and producing electricity. 354 MW of solar thermal electricity was installed in California in the 1980s.
Utility-Interactive Inverter	An inverter that can function only when tied to the utility grid, also called a grid-tied or grid-connected inverter.
Voltage	Electromotive force or potential difference, usually expressed in volts.
Watt (W)	The rate of energy transfer equivalent to one Ampere under one Volt. One Watt equals 1/746 horsepower, or one Joule per second. It is the product of Voltage and current.

*For a complete glossary of energy terms see the Energy Commissions **Consumer Energy Center Glossary** at: <http://www.consumerenergycenter.org/glossary/index.html>*